INSTITUTO SUPERIOR DE CIÊNCIAS DO TRABALHO E DA EMPRESA
FACULDADE DE CIÊNCIAS DA UNIVERSIDADE DE LISBOA

DEPARTMENTO DE FINANÇAS
DEPARTAMENTO DE MATEMÁTICA

American Options under Stochastic Volatility via a Transformation Procedure

João Miguel Mendes dos Reis

Mestrado em Matemática Financeira

Dissertação orientada por: Professor Doutor José Carlos Dias

2017

Resumo

Nesta tese explora-se o *pricing* the opções Americanas através de um *Transformation Procedure*, tendo por base o modelo de volatilidade estocástica de Heston. Dado que a informação empirica mostra que o preço das ações contém variações na sua volatilidade, principalmente devido ao denominado efeito de alavancagem, esta tese incorpora um processo estocástico para volatilidade além de para o processo do ativo subjacente, estando estes correlacionados, sendo que nos modelos mais simples é típico a volatilidade ser determinística. Para resolver a equação de derivadas parciais associada ao modelo de Heston um método de diferenças finitas é utilizado complementado por condições de fronteira apropriadas para uma opcção de venda. A utilização do método de diferenças finitas é instrumental para posteriormente através das suas partições no tempo conseguir que o preço seja solução para uma opção Americana, estando este sujeito a uma barreira-de-exercício, obtida através de um *Transformation Procedure* baseado na derivada da opção em relação ao seu preço, operando ao longo de várias iterações, contanto a tese com a prova de funcionalidade e uma ilustração deste *Transformation Procedure*. Esta tese também explora as condições de estabilidade numérica de acordo com a relação entre os parametros e as partições e também a precisão do método para diferentes partições das variáveis ao compará-lo com a solução de Heston para opções Europeias. Finalmente também é explorada a sensibilidade do preço das opções a diferentes variáveis, o efeito do preço quando introduzida a volatilidade estocástica face ao modelo determinístico e é explorada a eficiência face á precisão com a alteranção de diferentes parametros.

Abstract

Empirical data shows that volatility of asset prices is not constant, although the basic derivative pricing settings do not take this into account, and so stochastic volatility models are more capable of providing reliable asset prices. Pricing assets under stochastic volatility in American option setting provides a bigger challenge when compared to European option setting. This thesis attempts to provide prices for American options under stochastic volatility by first constructing a optimal exercise boundary followed by an asset price through a transformation procedure. First, the baseline European pricing model is constructed and tested for accuracy and numerical stability. Then the procedure is described, its guarantees for convergence are elaborated and the method is dessicated through an illustration. Lastly, the method is explored to give insights on how the option behaves when its parameters are changed, and its speed is tested in different computational settings.

Keywords:American options; stochastic volatility; free boundary

JEL Codes: G12, G13

Contents

List of Figures v

List of Tables vii

1. Numerical Method Overview 3
- 1.1. Stochastic Volatility Model . . . 3
- 1.2. Heston PDE Derivation . . . 7
- 1.3. Finite Differences Implementation . . . 11
- 1.4. Stability Testing . . . 17
- 1.5. Accuracy and Error Testing . . . 23

2. The Transformation Procedure 26
- 2.1. Method Summary . . . 26
- 2.2. Transformation Proofs . . . 27
  - 2.2.1. Base Theorem . . . 27
  - 2.2.2. Proof of Proposition 3.1 . . . 34
  - 2.2.3. Proof of Proposition 3.2 . . . 34
  - 2.2.4. Theorem 3.1 . . . 34
- 2.3. Illustration of the Procedure . . . 36
- 2.4. Results and benchmarking . . . 46

3. Parametrization insights 49
- 3.1. Stochastic volatility . . . 49
- 3.2. Correlation . . . 55
- 3.3. Market price of volatility . . . 56

4. Method efficiency and calibration 57
- 4.1. Partitioning . . . 57

4.2. Performance enhancement 58

5. Conclusions **61**

A. Matlab Code for American Options Through Transformation Procedure **62**

List of Figures

1.1. The continuation and stopping regions 5
1.2. Boundary conditions 6
1.3. Heston Grid 15
1.4. Numerical stability test 1 19
1.5. Numerical stability test 2 20
1.6. Numerical stability test 3 21
1.7. Numerical stability test 4 21
1.8. Numerical stability test 5 22
1.9. Numerical stability test 6 22
1.10. Accuracy test 1 24
1.11. Accuracy test 2 24
1.12. Accuracy test 3 25

2.1. Initial and Final exercise policies 37
2.2. Improvement sequence 38
2.3. First Iteration Sequence 1 39
2.4. First Iteration Sequence 2 39
2.5. First Iteration Sequence 3 40
2.6. First Iteration Sequence 4 40
2.7. First Iteration Sequence 5 40
2.8. First Iteration Sequence 6 41
2.9. First Iteration Sequence 7 41
2.10. First Iteration Sequence 8 41
2.11. First Iteration Sequence 9 42
2.12. First Iteration Sequence 10 42
2.13. First Iteration Sequence 11 42

2.14. First Iteration Sequence 12 43
2.15. First Iteration Sequence 13 43
2.16. Second Iteration Sequence 1 44
2.17. Second Iteration Sequence 2 44
2.18. Second Iteration Sequence 3 45
2.19. Second Iteration Sequence 4 45
2.20. Second Iteration Sequence 5 45
2.21. Second Iteration Sequence 6 46
2.22. Second Iteration Sequence 7 46
2.23. Comparison to the benchmark at $\gamma = 1$ 47

3.1. Price difference at $y = 0.2$ 50
3.2. Prices at $y = 0.2$ and $T = 0.250$ 50
3.3. Price difference at $y = 0.4$ 51
3.4. Prices at $y = 0.4$ and $T = 0.250$ 52
3.5. Price difference at $y = 0.6$ 53
3.6. Prices at $y = 0.6$ and $T = 0.250$ 54
3.7. Price and correlation 55
3.8. Price at Market Prices of Volatility 56

4.1. Price and γ factor 59
4.2. Exercise-Boundaries and γ 60

List of Tables

1.1. Base parameters stability 18
1.2. Model parameters stability 18
1.3. Partition parameters stability 18

2.1. Base parameters illustration 36
2.2. Model parameters illustration 36
2.3. Partition parameters illustration 36
2.4. Results table 47

4.1. Performance and partitioning 57
4.2. Performance and b^0 58
4.3. Performance and γ 59

Introduction

This thesis attempts to deal with a key feature in option pricing: the valuation of American options under stochastic volatility, while emulating the work of Chockalingam and Muthuraman (2011) [4].

Option contracts can be defined as European-style and American-style, with the former being able to be exercised only at the end of the agreed expiration date, and the latter at any point in time until the expiration date.[1] The American option pricing emerges as more nuanced, given the absence of a closed form solution even in the classical Black and Scholes (1973) [2] setting. This is mainly due to finding each optimal exercise point depends on the solution of the optimal exercise policy, where either the early exercise occurs, or the option is held, following the same progress of an European option, which allows us to interpret an American option as a succession of European options with different maturities.

In regards to volatility the classic models in the literature assume the presence of constant variance in the options' underlying asset value, which tends not to correspond to the empirical data, as several evidence points out to changes overtime, and negative correlation with asset prices. This is in part attributed to the leverage effect, that states that as the value of a firm's market equity decreases and debt remains constant and so its leverage increases, leading to higher risk and therefore increased volatility. This issue can be faced with various solutions, such as the one used in this thesis by assuming stochastic volatility correlated with the asset price, as achieved in Heston(1993)[7], and also by Hull and White (1987a)[8], Scott (1987)[14], Wiggins (1987)[16], Melino and Turnbull (1990, 1995)[12] [13] and Stein and Stein (1991)[15] or implementing a constant-elasticity-variance as Cox and Ross (1976)[6], and some models go even further such as Bates (1996)[1] which contemplates stochastic volatility complemented with jump-diffusion processes.

When it comes to American option pricing using the Heston model, various procedures based on finite differences have been used, such as the use of a discrete linear complementary

[1] In between these definitions, there is a Bermudan-style option, which can be exercised at a set of predetermined dates until the expiration date.

problem in Clarke and Parrot (1999)[5]. Ikonen and Tovainen study five different methods such as a Operator Splitting Method and a Penalty Method (2008a)[9] and also solve a linear complementarity problem through a two-dimensional parabolic partial differential equation (2008b)[10] and there is also the employment of Alternating Direction Implicit (ADI) schemes on non-uniform grids in Hout and Foulon (2010)[11].

To deal with the first issue, a stochastic volatility process will be assumed to be solved by a finite differences method, while for the second a transformation procedure based on the derivative of the underlying asset spot price is used.

The rest of the thesis is organized as follows:

Chapter 1 will develop and study the baseline Numerical Method; Section 1.1 formalizes the initial set-up of the model through the stochastic processes for the spot price and the volatility and the ancillary assumptions; in Section 1.2 the derivation of the Heston PDE is detailed; in Section 1.3 the Finite Differences method is built from the previous Sections' work; in Section 1.4 numerical stability is tested, and finally in Section 1.5 the accuracy of its output is verified.

Chapter 2 aims at extending the numerical method to deal with American options through the Transformation Procedure, summarizing it in section 2.1; develop its mathematical proofs in section 2.2; in section 2.3 an illustration is presented to dissect the inner workings of the Procedure, and in section 2.4 the result is compared to more conventional methods.

Chapter 3 uses the method to study the behaviour of American options when key parameters are altered. Section 3.1 deals with the inclusion of stochastic volatility, section 3.2 with correlation and section 3.3 with the market price of volatility.

Chapter 4 tests the method efficiency when the parameters are changed, section 4.1 studies the levels of partitioning and section 4.2 analyses the computation parameters of the initial exercise boundary and the tolerance value used in iteration.

1. Numerical Method Overview

1.1. Stochastic Volatility Model

As previously mentioned, an American option can be priced as a succession of European options with different maturities, so the first step is to simulate the European pattern of an option, what will be defined later as the *continuation region*, and to do so a finite differences method is employed.

Before applying the finite differences, it is necessary to set up the pricing method to derive the partial derivatives equation that will rule it, in this case the Heston PDE, known to capture stochastic volatility. The first step is to set up the stochastic processes described below.

The asset price S_t will be ruled by the geometric Brownian motion,

$$dS_t = rS_t dt + \sqrt{v_t} S_t dW_{1,t}, \tag{1.1}$$

with $W_{1,t}$ representing the standard Wiener process, $r > 0$ being the risk free rate, and $v > 0$ denoting instantaneous variance.

The mentioned volatility can follow its own process as intended in the Heston (1993) model, that is, the square root process

$$dv_t = \kappa(\theta - v_t)dt + \sigma\sqrt{v_t} dW_{2,t}, \tag{1.2}$$

with $W_{2,t}$ also being a standard Brownian Motion to be correlated with $W_{1,t}$, represented by $dW_{1,t}dW_{2,t} = \rho dt$, being constant as $\rho \in [-1, 1]$.

As for the other parameters, $\theta > 0$ is the long term mean of the instant variance, $\kappa > 0$ the speed of the regression to the mean, and $\sigma > 0$ the volatility of the variance process.

The choice of the parameters must respect the Feller condition: $\frac{2\kappa\theta}{\sigma} > 1$, which will ensure that a positive starting value for the instantaneous variance remains positive. Another important feature is the existence of the two separate random Brownian motions, and only one tradable asset, and so the market will be considered incomplete, with volatility not being a tradable asset.

After formulating the PDE that will rule the derivative price, the American option to be used must be formally defined. Considering a put option with an underlying asset defined as S_t, at time t defined by equation (1.1), the same underlying asset instantaneous volatility v_t at time t is represented by equation (1.2). Following the definition of a put option, that is, for a strike of K and maturity at T, a contract that allows the holder the right but not the obligation to sell the underlying asset at the value K, until T is reached for the American case, and so paying $(K - S_t)^+$. During this thesis the time to expiry of the option will be defined as $\tau \equiv T - t$, using also x as the asset price and y as the volatility, so the price of the put can be represented by $p(\tau, x, y)$.

By assuming, as usual, that the market selects a unique equivalent martingale measure $P^{*(\lambda)}$, for a unique market price of volatility, λ, the asset will be priced accordingly with:

$$p(\tau, x, y) = \sup_{\hat{\tau} \in (0,\tau)} E^{*(\lambda)}[e^{-r(\tau-\hat{\tau})}(K - S_{T-\hat{\tau}})^+ | S_\tau = x, Y_\tau = y]. \tag{1.3}$$

The optimal-exercise policy can be represented by a continuous, non-increasing surface $x = b(\tau, y)$, $b \in \mathbb{R}_+ \times \mathbb{R}_+ \to \mathbb{R}_+$. This boundary will separate two action regions: the *continuation region* where the optimal decision is to hold the American option, being defined as $C = \{(\tau, x, y) \in \mathbb{R}^2_+ \times \mathbb{R} | x > b(\tau, y)\}$ and the *stopping region*, where it is optimal do early exercise the American option, which is defined by $S = \{(\tau, x, y) \in \mathbb{R}^2_+ \times \mathbb{R} | x \leq b(\tau, y)\}$. As illustrated in figure 1.1, above the exercise boundary there is the stopping region, while below it there is the continuation region.

In the continuation region, the American option price follows the Heston PDE defined by:

$$\begin{aligned} &\frac{\partial U}{\partial t} + \frac{1}{2} v S^2 \frac{\partial^2 U}{\partial S^2} + \rho\sigma v S \frac{\partial^2 U}{\partial v \partial S} + \frac{1}{2}\sigma^2 v \frac{\partial^2 U}{\partial v^2} \\ &-rU + rS\frac{\partial U}{\partial S} + [\kappa(\theta - v) - \lambda(S, v, t)]\frac{\partial U}{\partial v} = 0. \end{aligned} \tag{1.4}$$

The derivation of the expression is presented in the following section. For convenience,

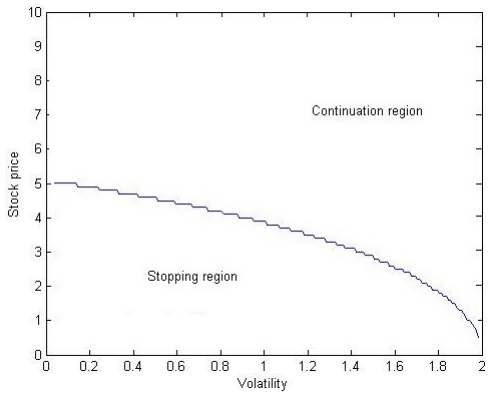

Figure 1.1.: The continuation and stopping regions

in this thesis Ł will represent the differential operator such that the previously presented Heston PDE can be represented by $Łp = 0$. Additional necessary ancillary conditions will be described below.

Firstly in the exercise region, the exercise payoff $p(\tau, x, y) = (K - x)^+$ for all $(\tau, x, y) \in Ł$.

In addition to the Heston PDE, the continuation and stopping regions need the following conditions to be solved:

• At maturity the only possible decision is to exercise the option:

$$p(0, x, y) = (K - x)^+. \tag{1.5}$$

• At the b frontier the payoff is the value of the early exercise:

$$p(\tau, b(\tau, y), y) = (K - b(\tau, y))^+. \tag{1.6}$$

• As the price tends to increasingly high values, the infinitesimal price change of the put tends to be null, due to being deep out-the-money:

$$\lim_{S \to \infty} \frac{\partial U}{\partial S} = 0. \tag{1.7}$$

• A similar argument applies, also when volatility is extremely large, small increases in it

tends to not affect the price, that is:

$$\lim_{y\to\infty} \frac{\partial U}{\partial y} = 0. \tag{1.8}$$

• When the volatility is zero, unlike in static volatility models, the price is not deterministic, and so the condition at $v = 0$ is obtained by inputing it in PDE (1.4), thus obtaining

$$A \equiv rx\frac{\partial U}{\partial x} + \kappa\theta\frac{\partial U}{\partial y} - rU - \frac{\partial U}{\partial t} = 0. \tag{1.9}$$

Using the Heston PDE and its ancillary conditions represented in figure 1.2, the American option is solved for a smooth surface optimal-exercise policy, which will be represented by b, and the *smooth pasting condition*, implying both p and $\frac{\partial p}{\partial x} = -1$ to be continuous across b, and it can be defined by $\lim_{x\downarrow b} \frac{\partial p}{\partial x} = -1$, that is, as x approaches b, the price variation of the put option will be proportional to the variation in the underlying asset price.

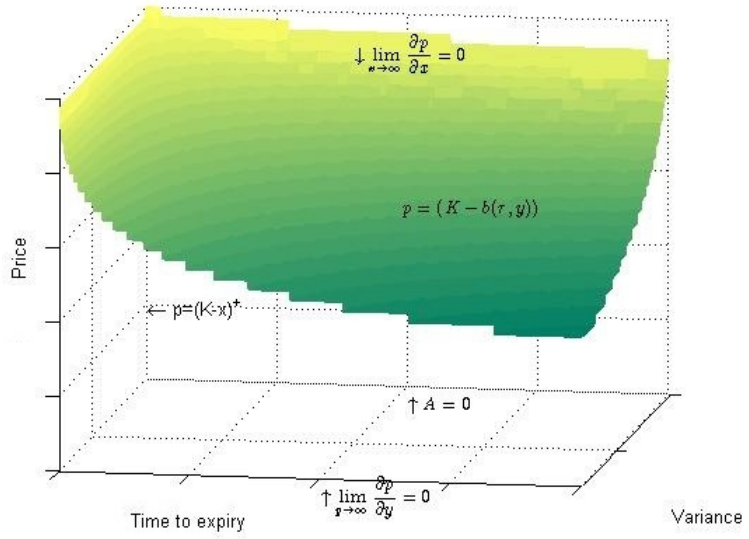

Figure 1.2.: Boundary conditions

1.2. Heston PDE Derivation

The argument to derive the Heston PDE is similar to the hedging argument for the Black-Scholes (1973) PDE, that is, a portfolio is formed with a derivative V, φ units of the underlying stock and in addition form the Black-Scholes model ϕ units of another option to hedge the volatility.

So having the portfolio with the value represent as

$$\Pi = V + \varphi S + \phi U. \tag{1.10}$$

Given that the portfolio is self financing, changes in value will be driven only by changes in its asset values:

$$d\Pi = dV + \varphi dS + \phi dU. \tag{1.11}$$

To solve dV, the Itô Lemma for two variables is used, reaching the following result:

$$dV(t, S_t, Y_t) = \frac{\partial V}{\partial t}dt + \frac{\partial V}{\partial S_t}dS_t + \frac{\partial V}{\partial v_t}dv_t + \frac{1}{2}\frac{\partial^2 V}{\partial S_t^2}(dS_t)^2 + \frac{1}{2}\frac{\partial^2 v}{\partial v_t^2}(dv_t)^2 + \frac{\partial^2 V}{\partial S_t \partial v_t}dS_t dv_t. \tag{1.12}$$

And given our initial definitions for S_t and v_t, then:

$$\begin{aligned} &(dS_t)^2 \\ &= (rS_t dt + \sqrt{v_t}S_t dW_{1,t})^2 \\ &= r^2 S_t^2 dt^2 + rS_t^2\sqrt{v_t}dtdW_{1,t} + v_t S_t^2 dW_{1,t}^2 \\ &= v_t S_t^2 dt, \end{aligned} \tag{1.13}$$

$$\begin{aligned} &(dv_t)^2 \\ &= (\kappa(\theta - v_t)dt + \sigma\sqrt{v_t}dW_{2,t})^2 \\ &= [\kappa(\theta - v_t)]^2 dt^2 + \kappa(\theta - v_t)\sigma\sqrt{v_t} \quad = dtdW_{2,t} + \sigma^2(\sqrt{v_t})^2 dW_{2,t}^2 \\ &= \sigma^2 v_t dt \end{aligned} \tag{1.14}$$

and

$$
\begin{aligned}
&dS_t dv_t \\
&= [rS_t dt + \sqrt{v_t} S_t dW_{1,t}][\kappa(\theta - v_t)dt + \sigma\sqrt{v_t} dW_{2,t}] \\
&= rS_t\kappa(\theta - v_t)dt^2 + rS_t\sigma\sqrt{v_t} d_t dW_{2,t} + \sqrt{v_t} S_t\kappa(\theta - v)dW_{1,t}dt + \sqrt{v_t}\sqrt{v_t} S_t\sigma dW_{1,t}dW_{2,t} \\
&= S_t\sigma v_t\rho dt,
\end{aligned}
\tag{1.15}
$$

since:

$$dt^2 = 0, \tag{1.16}$$

$$dtdW_{i,t} = 0 \tag{1.17}$$

and

$$(dW_{i,t})^2 = dt, \tag{1.18}$$

with $i \in \{1, 2\}$,which results in the following expression:

$$
\begin{aligned}
&dV(t, S_t, Y_t) \\
=&\frac{\partial V}{\partial t}dt + \frac{\partial V}{\partial S_t}dS_t + \frac{\partial V}{\partial v_t}dv_t + \frac{1}{2}\frac{\partial^2 V}{\partial S_t^2} v S_t^2 dt + \frac{1}{2}\frac{\partial^2 V}{\partial v_t^2}\sigma^2 v_t dt + \frac{\partial^2 V}{\partial S_t \partial v_t} S_t\sigma v_t\rho dt.
\end{aligned}
\tag{1.19}
$$

Using the same deduction for $dU(t, S_t, Y_t)$ the following expression is reached [1]:

$$\begin{aligned} d\Pi &= dV + \varphi dS + \phi dU \\ &= \left[\frac{\partial V}{\partial t} + \frac{1}{2}vS^2\frac{\partial^2 V}{\partial S^2} + \rho\sigma vS\frac{\partial^2 V}{\partial v \partial S} + \frac{1}{2}\sigma^2 v\frac{\partial^2 V}{\partial v^2}\right] dt \\ &+ \phi\left[\frac{\partial U}{\partial t} + \frac{1}{2}vS^2\frac{\partial^2 U}{\partial S^2} + \rho\sigma vS\frac{\partial^2 U}{\partial v \partial S} + \frac{1}{2}\sigma^2 v\frac{\partial^2 U}{\partial v^2}\right] dt \\ &+ \left[\frac{\partial V}{\partial S} + \phi\frac{\partial U}{\partial S} + \varphi\right] dS + \left[\frac{\partial V}{\partial v} + \phi\frac{\partial U}{\partial v}\right] dv. \end{aligned} \tag{1.20}$$

In order to have the portfolio only dependent on time, that is, not dependent on the spot price or volatility, the following two conditions will need to be satisfied:

$$\frac{\partial V}{\partial v} + \phi\frac{\partial U}{\partial v} = 0 \Leftrightarrow \phi = -\frac{\frac{\partial V}{\partial v}}{\frac{\partial U}{\partial v}} \tag{1.21}$$

and

$$\frac{\partial V}{\partial V} + \phi\frac{\partial U}{\partial S} + \varphi = 0 \Leftrightarrow \varphi = -\frac{\partial V}{\partial V} - \phi\frac{\partial U}{\partial S}, \tag{1.22}$$

thus resulting in the expression:

$$\begin{aligned} d\Pi &= \left[\frac{\partial V}{\partial t} + \frac{1}{2}vS^2\frac{\partial^2 V}{\partial S^2} + \rho\sigma vS\frac{\partial^2 V}{\partial v \partial S} + \frac{1}{2}\sigma^2 v\frac{\partial^2 V}{\partial v^2}\right] dt \\ &+ \phi\left[\frac{\partial U}{\partial t} + \frac{1}{2}vS^2\frac{\partial^2 U}{\partial S^2} + \rho\sigma vS\frac{\partial^2 U}{\partial v \partial S} + \frac{1}{2}\sigma^2 v\frac{\partial^2 U}{\partial v^2}\right] dt. \end{aligned} \tag{1.23}$$

Now given that the portfolio is riskless it can be assured that it will earn the risk free interest rate as time progresses, that is $d\Pi = r\Pi dt$, and by defining $r\Pi dt = r(V + \varphi S + \phi U)dt$ and combining (1.23) with the result from (1.10) and dividing by dt on both sides the following

[1] Omitting t in the notation

arises:

$$\begin{aligned}&\frac{\partial V}{\partial t}+\frac{1}{2}vS^2\frac{\partial^2 V}{\partial S^2}+\rho\sigma vS\frac{\partial^2 V}{\partial v\partial S}+\frac{1}{2}\sigma^2 v\frac{\partial^2 V}{\partial v^2}\\&+\phi\left[\frac{\partial U}{\partial t}+\frac{1}{2}vS^2\frac{\partial^2 U}{\partial S^2}+\rho\sigma vS\frac{\partial^2 U}{\partial v\partial S}+\frac{1}{2}\sigma^2 v\frac{\partial^2 U}{\partial v^2}\right]\\&=r(V+\varphi S+\phi U).\end{aligned}\tag{1.24}$$

Substituting with (1.21) and (1.22):

$$\begin{aligned}&\frac{\partial V}{\partial t}+\frac{1}{2}vS^2\frac{\partial^2 V}{\partial S^2}+\rho\sigma vS\frac{\partial^2 V}{\partial v\partial S}+\frac{1}{2}\sigma^2 v\frac{\partial^2 V}{\partial v^2}\\&-\frac{\frac{\partial V}{\partial v}}{\frac{\partial U}{\partial v}}\left[\frac{\partial U}{\partial t}+\frac{1}{2}vS^2\frac{\partial^2 U}{\partial S^2}+\rho\sigma vS\frac{\partial^2 U}{\partial v\partial S}+\frac{1}{2}\sigma^2 v\frac{\partial^2 U}{\partial v^2}\right]\\&=rV-\Big(-\frac{\partial V}{\partial S}-\Big(-\frac{\frac{\partial V}{\partial v}}{\frac{\partial U}{\partial v}}\Big)\frac{\partial U}{\partial S}\Big)rS-\frac{\frac{\partial V}{\partial v}}{\frac{\partial U}{\partial v}}rU.\end{aligned}\tag{1.25}$$

Putting all the elements in relation to V and U on each side of the equation through subtraction and division operations a new expression is reached:

$$\begin{aligned}&\frac{\left[\frac{\partial V}{\partial t}+\frac{1}{2}vS^2\frac{\partial^2 V}{\partial S^2}+\rho\sigma vS\frac{\partial^2 V}{\partial v\partial S}+\frac{1}{2}\sigma^2 v\frac{\partial^2 V}{\partial v^2}\right]-rV+rS\frac{\partial V}{\partial S}}{\frac{\partial V}{\partial v}}\\&=\frac{\left[\frac{\partial U}{\partial t}+\frac{1}{2}vS^2\frac{\partial^2 U}{\partial S^2}+\rho\sigma vU\frac{\partial^2 U}{\partial v\partial S}+\frac{1}{2}\sigma^2 v\frac{\partial^2 U}{\partial v^2}\right]-rU+rS\frac{\partial U}{\partial S}}{\frac{\partial U}{\partial v}}\quad.\end{aligned}\tag{1.26}$$

Now both sides depend only on one derivative, and so either of the sides can be represented by a function $f(S,v,t)$, applying Breeden(1979) [3] consumption model that specifies the price of volatility risk as a linear function of volatility (thus independent of the asset price), so that $\lambda(S,v,t)=\lambda v.$, with λ as a constant, then:

$$f(S,v,t)=-\kappa(\theta-v)+\lambda(S,v,t)\tag{1.27}$$

As mentioned in the previous chapter, since volatility cannot be traded in this incomplete market, it becomes necessary to estimate its price λ, with each estimation of λ corresponding

to a unique p^{λ} which results in the loss of price uniqueness, as different estimation procedures result in different prices for λ.

By substituting in (1.26) the left hand side dependent on V by the previous expression it results:

$$\begin{aligned} &-\kappa(\theta - v) + \lambda(S, v, t) \\ &= \frac{\left[\frac{\partial U}{\partial t} + \frac{1}{2} v S^2 \frac{\partial^2 U}{\partial S^2} + \rho\sigma v U \frac{\partial^2 U}{\partial v \partial S} + \frac{1}{2}\sigma^2 v \frac{\partial^2 U}{\partial v^2}\right] - rU + rS\frac{\partial U}{\partial S}}{\frac{\partial U}{\partial v}}. \end{aligned} \tag{1.28}$$

Finally by multiplying both sides by $\frac{\partial U}{\partial v}$ and isolating the right hand side the Heston PDE is reached:

$$\begin{aligned} &\frac{\partial U}{\partial t} + \frac{1}{2} v S^2 \frac{\partial^2 U}{\partial S^2} + \rho\sigma v U \frac{\partial^2 U}{\partial v \partial S} + \frac{1}{2}\sigma^2 v \frac{\partial^2 U}{\partial v^2} \\ &- rU + rS\frac{\partial U}{\partial S} + [\kappa(\theta - v) - \lambda(S, v, t)]\frac{\partial U}{\partial v} = 0. \end{aligned} \tag{1.29}$$

1.3. Finite Differences Implementation

The Heston PDE can be solved into a closed form solution, expressed in terms of characteristic functions, as in Heston (1993) to price an European option, but for the American case it is convenient to have the time partitioning in order to check the early exercise decision. To do so, a first differences method is used.

The first step to obtain the numerical values is to truncate the variables in intervals $[0, \hat{T}]$, with $\hat{T}$ representing the last time to maturity to obtain the values, $[0, \hat{X}]$, which in this thesis is going to be $2 \times K$, with K being the underlying asset strike, and $[0, \hat{Y}]$, which in this thesis for the sake of covering a wide range of values will be $\hat{Y} = 2$.

Then the three variables will be uniformly divided, by l, m, n, with $\delta_t = \frac{\hat{T}}{l}$, $\delta_x = \frac{\hat{X}}{m}$ and $\delta_y = \frac{\hat{Y}}{n}$, yielding the points $k = 0, ..., l$, $i = 0, ..., m$ and $j = 0, ..., n$, with respectively $l + 1$, $m + 1$ and $n + 1$ points, which will allow us to denote $p(\delta_t k, \delta_x i, \delta_y j) = p(\tau_k, x_i, y_j) = p^k_{i,j}$.

Picking the Heston PDE from the previous section, the λ parameter is set as $\lambda(S, v, t) \equiv$

$\sigma\sqrt{y}\lambda$, resulting in[2]:

$$\frac{\partial U}{\partial t}+\frac{1}{2}yS^2\frac{\partial^2 U}{\partial S^2}+\rho\sigma yS\frac{\partial^2 U}{\partial S\partial y}+\frac{1}{2}\sigma^2 y\frac{\partial^2 U}{\partial y^2}+rS\frac{\partial U}{\partial S}+[\kappa(\theta-y)-\sigma\sqrt{y}\lambda]\frac{\partial U}{\partial y}-rU=0. \quad (1.30)$$

Manipulating the first term and applying the Euler method, substituting time since inception t by to time to maturity τ having $dt=-d\tau$, which will change index $k+1$ to index k, and k to $k-1$ one obtains:

$$\frac{\partial U}{\partial t}=\frac{p^{k+1}-p^k}{\delta t}=-\frac{p^k-p^{k-1}}{\delta\tau} \quad (1.31)$$

Isolating the term from the previous expression, while replacing the other terms defined by the central derivatives expressed as:

$\partial U/\partial S=\big(p^k_{i+1,j}-p^k_{i-1,j}\big)/2\delta_x$,

$\partial U/\partial y=(p^k_{i,j+1}-p^k_{i,j-1})/2\delta_y$,

$\partial^2 U/\partial S^2=(p^k_{i+1,j}-2p^k_{i,j}+p^k_{i-1,j})/\delta_x^2$,

$\partial^2 U/\partial y^2=(p^k_{i,j+1}-2p^k_{i,j}+p^k_{i,j-1})/\delta_y^2$,

and

$\partial^2 U/\partial y\partial S=(p^k_{i+1,j+1}-p^k_{i-1,j+1}-p^k_{i+1,j-1}+p^k_{i-1,j-1})/4\delta_x\delta_y$

then,

$$\begin{aligned}\frac{p^k_{i,j}-p^{k-1}_{i,j}}{\delta_\tau}&=\frac{1}{2}yS^2\Big(\frac{p^k_{i+1,j}-2p^k_{i,j}+p^k_{i-1,j}}{\delta_x^2}\Big)+\Big(\rho\sigma yS\frac{p^k_{i+1,j+1}-p^k_{i-1,j+1}-p^k_{i+1,j-1}+p^k_{i-1,j-1}}{4\delta_x\delta_y}\Big)\\&+\frac{1}{2}\sigma^2 y\Big(\frac{p^k_{i,j+1}-2p^k_{i,j}+p^k_{i,j-1}}{\delta_y^2}\Big)+rS\Big(\frac{p^k_{i+1,j}-p^k_{i-1,j}}{2\delta_x}\Big)\\&+[\kappa(\theta-y)-\sigma\sqrt{y}\lambda]\Big(\frac{p^k_{i,j+1}-p^k_{i,j-1}}{2\delta_y}\Big)-rp^k_{i,j}.\end{aligned} \quad (1.32)$$

[2]With y replacing v in the representation of volatility.

Separating the terms and isolating the right hand side,

$$\begin{aligned}
&\frac{yS^2}{2\delta_x^2}p_{i+1,j}^k - \frac{yS^2}{\delta_x^2}p_{i,j}^k + \frac{yS^2}{2\delta_x^2}p_{i-1,j}^k \\
&+ \rho\sigma yS\frac{p_{i+1,j+1}^k}{4\delta_x\delta_y} - \rho\sigma yS\frac{p_{i-1,j+1}^k}{4\delta_x\delta_y} - \rho\sigma yS\frac{p_{i+1,j-1}^k}{4\delta_x\delta_y} + \rho\sigma yS\frac{p_{i-1,j-1}^k}{4\delta_x\delta_y} \\
&+ \frac{1}{2}\sigma^2 y\frac{p_{i,j+1}^k}{\delta_y^2} - \sigma^2 y\frac{p_{i,j}^k}{\delta_y^2} + \frac{1}{2}\sigma^2 y\frac{p_{i,j-1}^k}{\delta_y^2} \\
&\frac{rS}{2}\frac{p_{i+1,j}^k}{\delta_x} - \frac{rS}{2}\frac{p_{i-1,j}^k}{\delta_x} + \frac{[\kappa(\theta-y)-\sigma\sqrt{y}\lambda]}{2\delta_y}p_{i,j+1}^k \\
&- \frac{[\kappa(\theta-y)-\sigma\sqrt{y}\lambda]}{2\delta_y}p_{i,j-1}^k - rp_{i,j}^k - \frac{p_{i,j}^k}{\delta_t} + \frac{p_{i,j}^{k-1}}{\delta_t} = 0 \qquad .
\end{aligned} \tag{1.33}$$

and aggregating by grid point from previous timestep used:

$$\begin{aligned}
&\Big(\frac{1}{2}\frac{yS^2}{\delta_x^2} + \frac{rS}{2\delta_x}\Big)p_{i+1,j}^k + \Big(-\frac{\rho\sigma yS}{4\delta_x\delta_y}\Big)p_{i-1,j+1}^k + \Big(\frac{1}{2}\frac{\sigma^2 y}{\delta_y^2} + \frac{[\kappa(\theta-y)-\sigma\sqrt{y}\lambda]}{2\delta_y}\Big)p_{i,j+1}^k \\
&+ \frac{\rho\sigma yS}{4\delta_x\delta_y}p_{i+1,j+1}^k + \frac{\rho\sigma yS}{4\delta_x\delta_y}p_{i-1,j-1}^k + \Big(\frac{1}{2}\frac{\sigma^2 y}{\delta_y^2} - \frac{[\kappa(\theta-y)-\sigma\sqrt{y}\lambda]}{2\delta_y}\Big)p_{i,j-1}^k \\
&+ \Big(-\frac{\rho\sigma yS}{4\delta_x\delta_y}\Big)p_{i+1,j-1}^k + \Big(\frac{1}{2}\frac{yS^2}{\delta_x^2} - \frac{rS}{2\delta_x}\Big)p_{i-1,j}^k + \Big(-\frac{yS^2}{\delta_x^2} - \frac{\sigma^2 y}{\delta_y^2} - r - \frac{1}{\delta_\tau}\Big)p_{i,j}^k = -\frac{p_{i,j}^{k-1}}{\delta_\tau}.
\end{aligned} \tag{1.34}$$

Substituting $S = i \times \delta_x$ and $y = j \times \delta_y$, and grouping alike terms,

$$\begin{aligned}
&\Big(\frac{1}{2}\frac{j\delta_v(i\delta_x)^2}{\delta_x^2} + \frac{ri\delta_x}{2\delta_x}\Big)p^k_{i+1,j} + \Big(\frac{\rho\sigma j\delta_y i\delta_x}{4\delta_x\delta_y}\Big)\Big(- p^k_{i-1,j+1} - p^k_{i+1,j-1} + p^k_{i+1,j+1} + p^k_{i-1,j-1}\Big)\\
&+ \Big(\frac{1}{2}\frac{\sigma^2 j\delta_y}{\delta_y^2} + \frac{[\kappa(\theta - j\delta_y) - \sigma\sqrt{j\delta_y}\lambda]}{2\delta_y}\Big)p^k_{i,j+1}\\
&+ \Big(\frac{1}{2}\frac{\sigma^2 j\delta_y}{\delta_y^2} + \frac{[\sigma\sqrt{j\delta_y}\lambda - \kappa(\theta - j\delta_y)]}{2\delta_y}\Big)p^k_{i,j-1}\\
&+ \Big(\frac{1}{2}\frac{j\delta_y(i\delta_x)^2}{\delta_x^2} - \frac{ri\delta_x}{2\delta_x}\Big)p^k_{i-1,j}\\
&+ \Big(- \frac{j\delta_y(i\delta_x)^2}{\delta_x^2} - \frac{\sigma^2 j\delta_y}{\delta_y^2} - r - \frac{1}{\delta_\tau}\Big)p^k_{i,j} = -\frac{p^{k-1}_{i,j}}{\delta_\tau}.
\end{aligned} \tag{1.35}$$

By multiplying both sides by $-\delta_\tau$ and clearing fraction terms, the following arises by separating each price term:

$$\begin{aligned}
T_1 &= -\frac{\rho\sigma ji\delta_\tau}{4}\\
T_2 &= \frac{\kappa\theta\delta_\tau}{2\delta_y} - \frac{\sigma^2 j\delta_\tau}{2\delta_y} - \frac{\kappa j\delta_\tau}{2} - \frac{\sigma\sqrt{j}\lambda\delta_\tau}{2\sqrt{\delta_y}}\\
T_3 &= \frac{\rho\sigma ji\delta_\tau}{4}\\
T_4 &= \frac{ri\delta_\tau}{2} - \frac{j\delta_y i^2\delta_\tau}{2}\\
T_5 &= 1 + r\delta_\tau + ji^2\delta_\tau\delta_y + \sigma^2 j\frac{\delta_\tau}{\delta_y}\\
T_6 &= -\frac{j\delta_y i^2\delta_\tau}{2} - \frac{ri\delta_\tau}{2}\\
T_7 &= \frac{\rho\sigma ji\delta_\tau}{4}\\
T_8 &= -\frac{\kappa\theta\delta_\tau}{2\delta_y} - \frac{\sigma^2 j\delta_\tau}{2\delta_y} + \frac{\kappa j\delta_\tau}{2} + \frac{\sigma\sqrt{j}\lambda\delta_\tau}{2\sqrt{\delta_y}}\\
T_9 &= -\frac{\rho\sigma ji\delta_\tau}{4}.
\end{aligned} \tag{1.36}$$

Then:

$$p^k_{i-1,j-1}T_1 + p^k_{i,j-1}T_2 + p^k_{i+1,j-1}T_3 + p^k_{i-1,j}T_4 + p^k_{i,j}T_5 \\ +p^k_{i+1,j}T_6 + p^k_{i-1,j+1}T_7 + p^k_{i,j+1}T_8 + p^k_{i+1,j+1}T_9 = p^{k-1}_{i,j}. \tag{1.37}$$

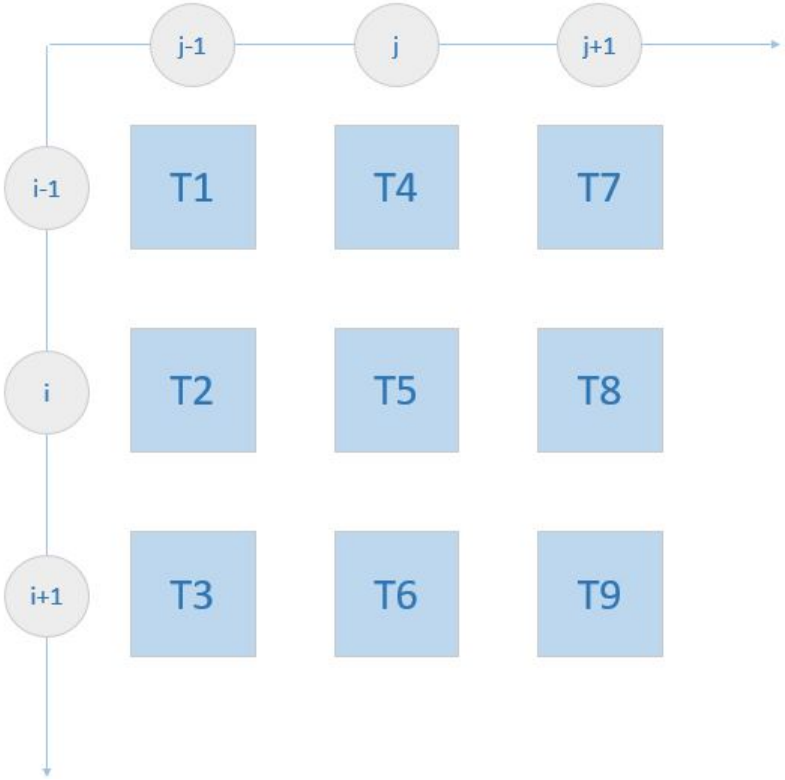

Figure 1.3.: Heston PDE grid for $p_{i,j}$

As highlighted in figure 1.3, while the last equation provides solutions for values in the grid as long they are surrounded by points in all the other directions, giving nine values from $\tau - 1$ to feed into $p^\tau_{i,j}$, there are limitations when they are at one of the four borders, the maxima and minima of S and y.

The $y = 0$ border can have its own equation, being the previous condition for $y = 0$, solved so in a very similar way to the full Heston PDE

$$rS\frac{\partial U}{\partial S} + \kappa\theta\frac{\partial U}{\partial y} - rp - \frac{\partial U}{\partial t} = 0. \tag{1.38}$$

Next S and t are treated in the same way as in the former expression. In the case of y the substitution is done by the forward derivatives, since it is not possible to incorporate negative volatility. Hence:

$$\begin{aligned}
&rS\Big(\frac{p^k_{i+1,j}-p^k_{i-1,j}}{2\delta_x}\Big)+\kappa\theta\Big(\frac{p^k_{i,j+1}-p^k_{i,j}}{\delta_y}\Big)-rp^k_{i,j}-\frac{p^k_{i,j}-p^{k-1}_{i,j}}{\delta_\tau}=0\\
&\frac{rS}{2\delta_x}p^k_{i+1,j}-\frac{rS}{2\delta_x}p^k_{i-1,j}+\frac{\kappa\theta}{\delta_y}p^k_{i,j+1}-\frac{\kappa\theta}{\delta_y}p^k_{i,j}-rp^k_{i,j}-\frac{p^k_{i,j}}{\delta_\tau}+\frac{p^{k-1}_{i,j}}{\delta_\tau}=0\\
&p^{k-1}_{i,j}=\frac{rS}{2}\frac{\delta_t}{\delta_x}p^k_{i-1,j}+p^k_{i,j}+r\delta_t p^k_{i,j}-\frac{rS}{2}\frac{\delta_t}{\delta_x}p^k_{i+1,j}-\kappa\theta\frac{\delta_t}{\delta_y}p^k_{i,j+1}+\kappa\theta\frac{\delta_t}{\delta_y}p^k_{i,j}
\end{aligned}\tag{1.39}$$

so

$$p^{k-1}_{i,j}=\frac{rS}{2}\frac{\delta_t}{\delta_x}p^k_{i-1,j}+\Big(1+r\delta_t+\kappa\theta\frac{\delta_t}{\delta_y}\Big)p^k_{i,j}-\frac{rS}{2}\frac{\delta_t}{\delta_x}p^k_{i+1,j}-\kappa\theta\frac{\delta_t}{\delta_y}p^k_{i,j+1}.\tag{1.40}$$

After arranging in similar fashion as before and then substituting $S=i\times\delta_x$, then

$$p^{k-1}_{i,j}=\frac{ri}{2}\delta_t p^k_{i-1,j}-\frac{ri}{2}\delta_t p^k_{i+1,j}+\Big(1+r\delta_t+\kappa\theta\frac{\delta_t}{\delta_y}\Big)p^k_{i,j}-\kappa\theta\frac{\delta_t}{\delta_y}p^k_{i,j+1}.\tag{1.41}$$

While for the value at $y=0$ the latter expression is able to dismiss values to its left, there are still issues at the remaining borders, and the conditions defined in section 2.1 chapter come into use.

- For the s boundary at $\hat{X}$ the $\lim_{S\to\infty}\frac{\partial U}{\partial S}=0$ condition is used, yielding

$$p^k_{i,j}=p^k_{i-1,j},\tag{1.42}$$

so when $i=m$, that is the last grid point in the S axis it is a copy of the previous one.

- The boundary at $\hat{Y}$ the $\lim_{y\to\infty}\frac{\partial U}{\partial y}=0$ is used alike for the $\hat{X}$ case, with

$$p^k_{i,j}=p^k_{i,j-1},\tag{1.43}$$

when $j=n$ the procedure is similar to $i=m$.

• With respect to the border where $S = 0$, the put option would be immediately exercised, as it reaches the maximum possible payoff

$$p^{\tau}_{0,y} = K. \tag{1.44}$$

• As for the *stopping* region the condition, i.e. $S_i \leq b(\tau_k, y_j)$, the early exercise payoff will always be:

$$p^{k}_{i,j} = (K - \delta_x i)^+. \tag{1.45}$$

• Finally the last condition at $\tau = 0$ will provide the starting values for the method to start progressing

$$p^{0}_{i,j} = (K - \delta_x i)^+. \tag{1.46}$$

So for a given price $p^{k-1}_{i,j}$ $\forall i, j$ the price at time to expiry τ_{k-1} can be obtained by the values at τ_k, which can be expressed as $\boldsymbol{p^{k-1}} = T\boldsymbol{p^{k}}$, where T represents the PDE expressions mentioned above, and $\boldsymbol{p^{k-1}}$ vector of the values to be deduced and $\boldsymbol{p^{k}}$ the previous period known values, which can be complemented later with an exercise policy $\boldsymbol{b}$.

1.4. Stability Testing

A common challenge when using numerical methods is the stability of the method, that is, the capacity of the method to converge into viable values, avoiding the development and posterior amplification and diffusion of errors, which prevent the effective use of the method to provide results.

The stability will depend on the model parameters chosen, which must be matched by an adequate partition level through the adequate choice of l, m and n. While m and n tend to be chosen to obtain accuracy, the posterior choice of l must accommodate to achieve stability.

For the sake of testing stability a European option will be assumed, that is without including the early exercise boundary. The stability in a European setting is required to evaluate the American option, and once achieved the introduction of the exercise-boundary $\mathbf{b}$ will not compromise it.

So for various levels of partitioning the parameters from Tables 1.1 to 1.3 the method will be tested:

$\hat{T}$ - Time to expiry maximum	0.125
$\hat{X}$ - Spot maximum	20
$\hat{Y}$ - Volatility maximum	2
K - Strike	10

Table 1.1.: Base parameters.

r - Interest rate	2%
κ - Volatility speed of reversion	3
θ - Long term variance	0.2
σ - Volatility of variance	0.5
ρ - Spot/Volatility correlation	-0.1

Table 1.2.: Model parameters.

l - Time partition	100
m - Spot partition	40
n - Volatility partition	40

Table 1.3.: Partition parameters.

Many of the following outputs acquired humongous absolute values, due to the difficulty to graph the huge output values of such scale, a logarithmic scale was introduced, and to be able to use this logarithmic scale with negative numbers the minimum term in each grid was added in absolute value to all the output before applying the logarithm. All the cases where the adapted logarithmic scale is not used are properly mentioned. The horizontal axis in the following figures present the point in the grid, opposed to the true values of the spot and volatility.

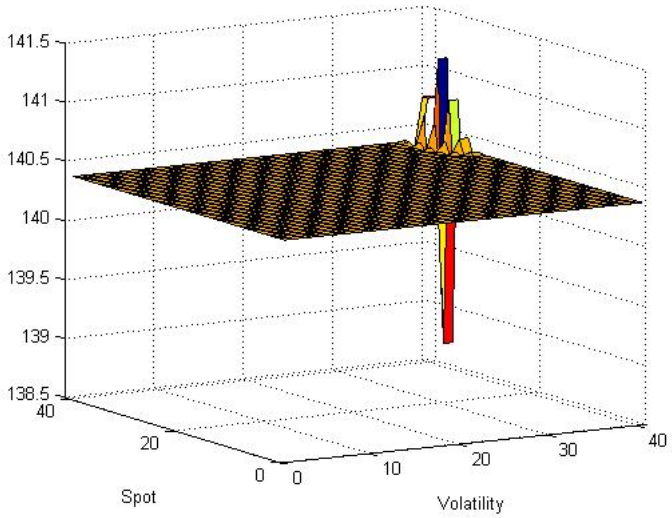

Figure 1.4.: $T = 0.125$, $l = 100$, $m = 40$, $n = 40$

As depicted in figure 1.4 the returned price result is erratic, with very wide swings in values, both huge negative and positive values, which clearly violate the restrictions that the put option maximum value should be its Strike and that its value cannot be negative. The generator of erratic behaviour is the area of higher price and volatility, whose error is propagated through τ, although the invalidity of the output is not consistent, as displayed in the graphs below, that provided the first $x \times y$ grid point values.

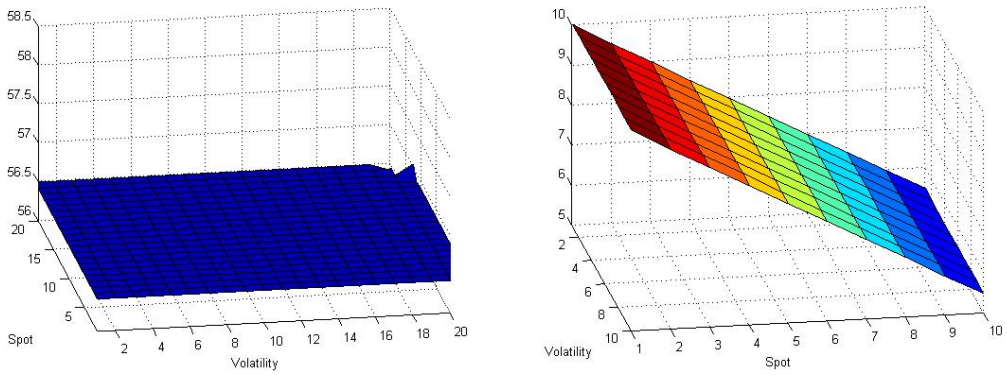

(a) 21x21 (b) 10x10 - Non logaritmic

Figure 1.5.: $T = 0.125$, $l = 100$, $m = 40$, $n = 40$

As figure 1.5 displays even though at different scales, across almost all the output the values are not viable. Although looking first ten per ten grid points, the values are in an acceptable range considering the values a put option can assume, but still the values at that range might be biased due to the effect of the erratic values over the rest of the grid, and that bias finds greater expression as the τ progresses. For a clearer representation if the same parameters are for larger time periods while holding δ_τ eventually the whole grid will assume erratic values, as can be observed if now we assume $\hat{T} = 0.250$ and $l = 200$.

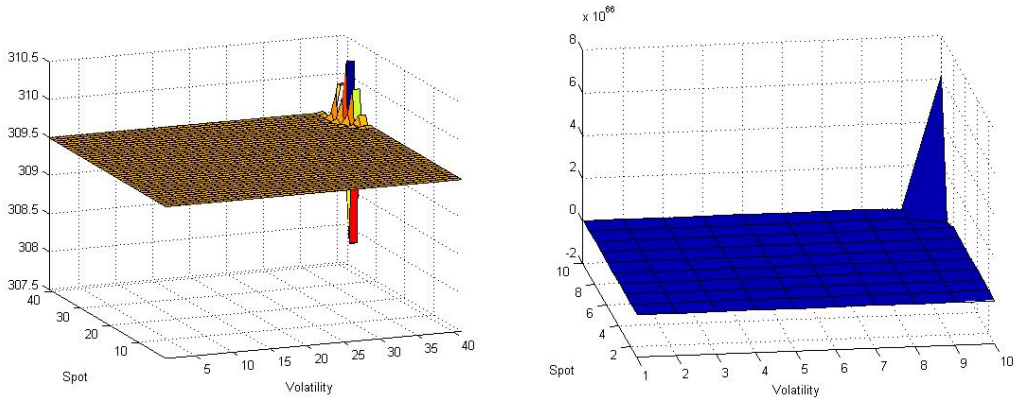

(a) 40x40 (b) 10x10 - Non logaritmic scale

Figure 1.6.: $T = 0.250$, $l = 200$, $m = 40$, $n = 40$

As observed in figure 1.6, as the same parameters are carried through time from $\tau = 0.125$ to $\tau = 0.250$, duplicating the l to keep δ_t constant, the graph of the grid as a whole displays a similar shape, although the first ten per ten points now clearly display unreasonable values.

Back to the first maturity value $\tau = 0.125$, by increasing to $l = 200$, the following is obtained.

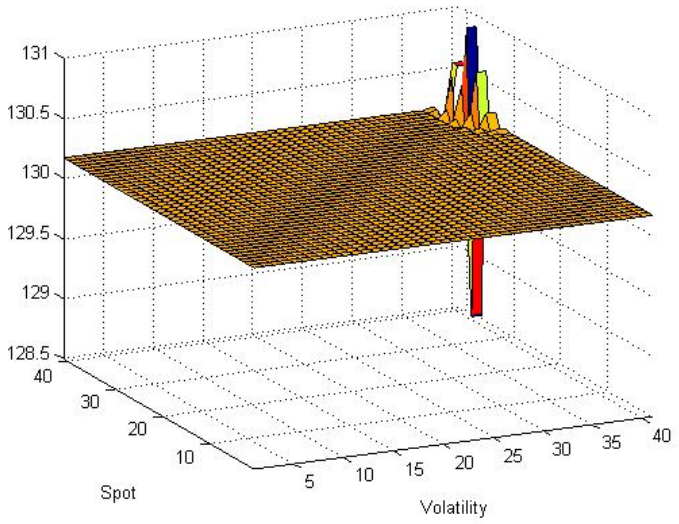

Figure 1.7.: $T = 0.125$, $l = 200$, $m = 40$, $n = 40$

With the increase in l to 200 in the partitions the values are less disproportional but still unsatisfactory for the overall grid.

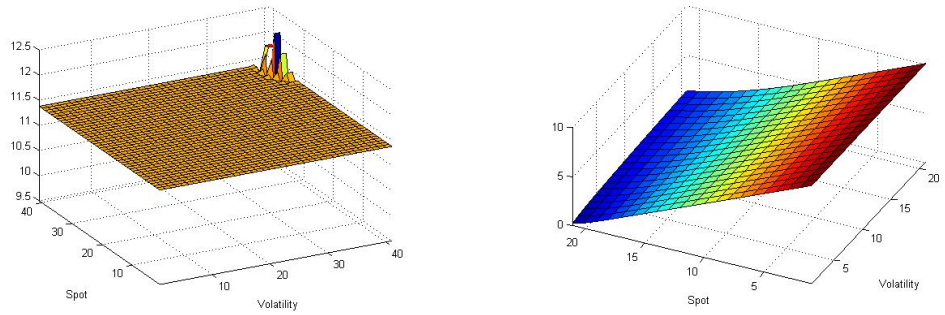

(a) 41x41 (b) 21x21 - Non logaritmic scale

Figure 1.8.: $T = 0.125$, $l = 300$, $m = 40$, $n = 40$

Further increasing the partitions, with $l = 300$ figure 1.8 shows the overall values are still inadequate, although now focusing in the first quadrant of the matrix, most of the values fit what one would expect from a put option.

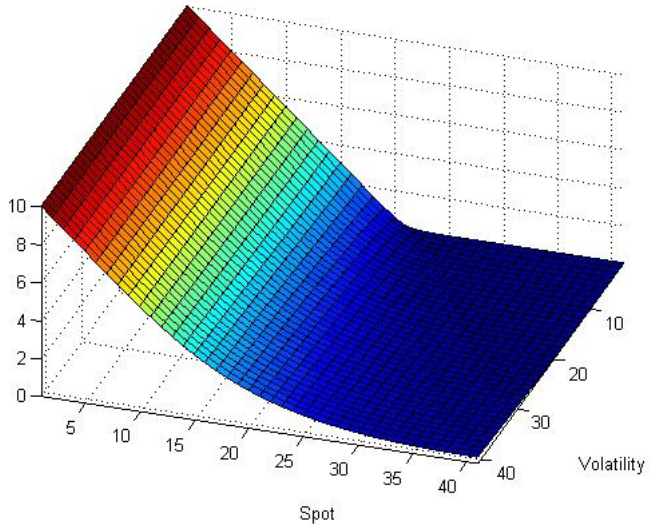

Figure 1.9.: $T = 0.125$, $l = 400$, $m = 40$, $n = 40$ - non logarithmic

Finally, with the value of $l = 400$ in the partitions and reaching a $\delta_\tau = 3.1250e - 04$, the

value of the put option price in figure 1.9 has reached stability across the whole grid, and so completing a necessary condition to use the numerical method.

1.5. Accuracy and Error Testing

In the finite differences method, even when under numerical stability, a difference between the result and the true value may exist. This can be justified by the truncation error, given that the values of the derivatives arise on an approximation of an infinite sum through a finite sum based on Taylor's approximations. In this section the dimension of such error and its mitigation through increasing partitions are studied through numerical testing.

Although for the further study of American options a closed formula cannot be used, it is possible to use a closed form for the Heston model for European options which can be compared to the baseline first differences European model. Despite the closed form of the Heston model also using a numerical method to integrate its probabilities, a comparison between the closed formula and the finite differences can deliver insights.

The parameters selected for testing are the same as the ones used in the previous stability analysis section.

It is important to analyse the evolution of the numerical method as the number of space partitions increases, while keeping time partitioning constant at $l = 1000$; further the number of divisions in the spot and volatility ranges from 10 to 60, with additional 10 divisions per test. The figures below show the progression with the solid line representing the closed form and the dashed line points for the finite differences.

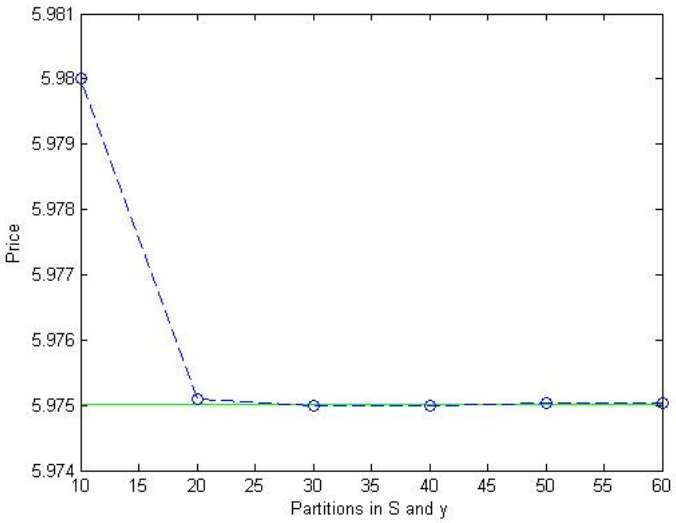

Figure 1.10.: Spot= 4, Volatility= 0.4

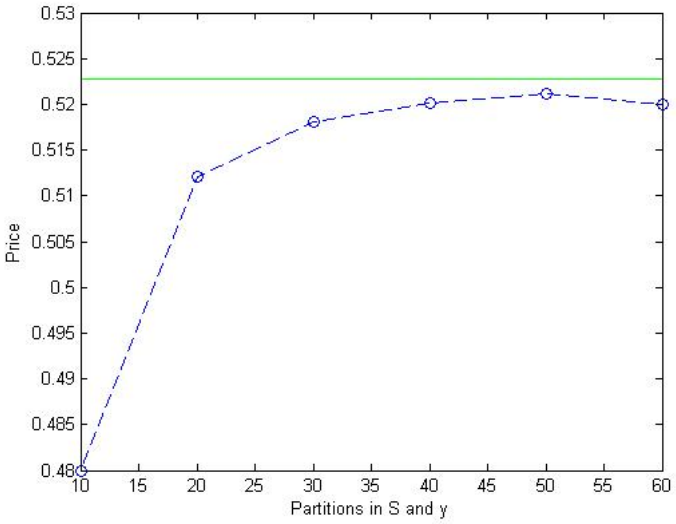

Figure 1.11.: Spot= 12, Volatility= 0.8

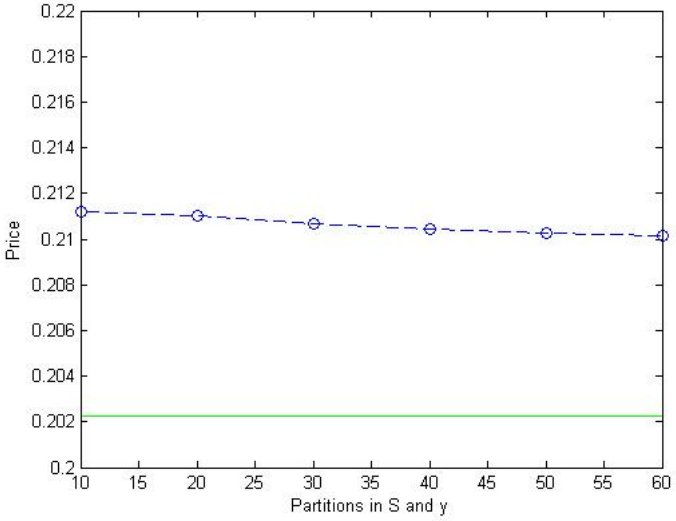

Figure 1.12.: Spot= 16, Volatility= 1.2.

To sum up, in all partition levels the difference between the closed form price and the finite differences tends to be small, in a few fraction of cents range. In general the difference is reduced as the partitions increase, as in the first case, although some increases may not always reduce the gap as in the second case, while cases such as the third when the partitions are increased the prices tend to the Heston closed form, although keeping some distance. Overall, both forms tend to provide similar results, despite some nuanced cases.

2. The Transformation Procedure

2.1. Method Summary

All the demonstrations referring to the propositions in this section are displayed in the next section.

The Transformation Procedure to be presented and demonstrated will allow the free-boundary problem to be solved, revealing the optimal-exercise barrier, and so separating the *continuation* and *stopping* regions.

It can be defined that the Heston PDE and the ancillary conditions are satisfied by a price function $p(\tau, x, y)$ given the optimal-exercise policy represented by $b(\tau, y)$, and for a given arbitrary policy represented by $b^0(\tau, y)$ associated with price function represented by $p^0(\tau, x, y)$, which will respect $p^0(\tau, x, y) = p(\tau, x, y)$ when $b^0 = b$ and $p^0(\tau, x, y) \leq p(\tau, x, y)$ for any other b^0.

Given a b^0 policy, its value can be calculated using a numerical method to solve the Heston PDE, being detailed in section 2.3, with the uniqueness of the value function being guaranteed by Proposition 3.1.

Proposition 3.1: If p^n satisfies the Heston PDE and the attached conditions, a given $b^n(\tau, y)$ generates a unique p^n.

The Transformation Procedure will aim to converge and generate an optimal price. Starting at b^0 a sequence b^0, b^1,..., b that respects $b^n(\tau, y) < b^{n+1}(\tau, y)$ for all (τ, y) is guaranteed to converge, and while so $p^n(\tau, x, y) < p^{n+1}(\tau, x, y)$ for all (τ, x, y).

In order to progress through the b^n sequence, the following condition is necessary:

$$\frac{\partial p^0}{\partial x}|_{(\tau, b^0(\tau, y)+, y)} < -1. \tag{2.1}$$

Due to Proposition 3.2 it will be assured that a suboptimal policy below b will respect the condition, as long a $b^0 < b$ is chosen. The initial choice for b^0 tends to be of easy to guess

through picking a low value.

Proposition 3.2: If $b^0(\tau, y) < b(\tau, y)$, then $\frac{\partial p^0}{\partial x}|_{(\tau, b^0(\tau,y)+, y)} < -1$.

After selecting a policy b^0 its conditions are solved for the *continuation* and *stopping* regions and p^0 is obtained, over the boundary represented by $x = b^0$, it will be verified that $p^0 = (K - x)^+$, and immediately above b^0 the derivative with respect to x will be below -1, in accordance with $p^0 < (K - x)^+$. So by expanding the *stopping* region there will be a policy improvement, and so by selecting a new policy $b^1 > b^0$ the payoff will approach optimality.

In order to keep iterating it is also convenient, that b^1 is still below b, i.e., a boundary where an infinitesimal increase in the price x still leads to a less than proportional increase in the price, which will be represented by the expression:

$$b^{n+1}(\tau, y) = \left\{ \sup_{b^n(\tau,y)} x \quad \frac{\partial p^n}{\partial x}|_{(\tau,x,y)} < -1 \right\}. \tag{2.2}$$

The existence of this will be guaranteed by the theorem that follows, as long as we are still below $p^n = (K - x)^+$, which also guarantees that the p^{n+1} is greater than p and can be iterated from the latter boundary.

Theorem 3.1: If $p^n \in C^{1,2}$ solves the Heston PDE and ancillary conditions, while having $\frac{\partial p^n}{\partial x}|_{(\tau, b^n(\tau,y)+, y)} < -1$, then the b^{n+1} exists. In addition the price function p^{n+1} obtained using b^{n+1} is such that $p^{n+1} > p^n$ and $\frac{\partial p^{n+1}}{\partial x}|_{(\tau, b^{n+1}(\tau,y)+, y)} < -1$.

By picking successive policies using the condition (2.1), eventually the *smooth pasting condition* will be reached, and yielding an optimal result with $p(\tau, x, y)$ and $b(\tau, x, y)$.

2.2. Transformation Proofs

This section contains the detailed proofs of the original publication in Appendix A, with a extended version of abbreviated proofs.

The first theorem demonstration will prove a maxima and minima set result that will be instrumental in subsequent proofs.

2.2.1. Base Theorem

The Theorem states that:

For $\hat{T} \in (0,\infty)$, and a continuous $g(\tau, y) > 0$ that will represent spot prices, for all $(\tau, y) \in (0, \hat{T}) \times \mathbb{R}_+$, as in the early sections let the *continuation* region be defined $\hat{C} = \{(\tau, x, y) \in (0, \hat{T}) \times \mathbb{R}^2_+ \mid x > g(\tau, y)\}$. In addition let H be the price solution to $ŁH = 0$ in $\hat{C}$, with the following conditions:

At $\tau = 0$, the option's expiry date the value will be null at the *continuation* region, it will be worthless not to exercise, that is

$$H(0, x, y) = 0. \tag{2.3}$$

At a given point in the exercise border the value of H will be represented by a positive F function.

$$H(\tau, g(\tau, y), y) = F(\tau, y) \ > 0. \tag{2.4}$$

As seen before when defining the stochastic model at very high values of price and variance, its fluctuations do not affect the put option's price. Therefore,

$$\lim_{x \to \infty} \frac{\partial H}{\partial x} = 0 \tag{2.5}$$

and

$$\lim_{y \to \infty} \frac{\partial H}{\partial y} = 0. \tag{2.6}$$

At $y = 0$, as seen previously, this condition will rule our expression when the volatility is null:

$$rx\frac{\partial H}{\partial x} + \kappa\theta - rH - \frac{\partial H}{\partial t} = 0. \tag{2.7}$$

Given the above, if $r > 0$ and $F(\tau, y) > 0$ for all $(\tau, y) \in (0, \hat{T}) \times \mathbb{R}_+$, then the maxima of H are attained only on the boundary $(\tau, g(\tau, y), y)$ and the minima on the boundary $(0, x, y)$.

Proof:

The proof will start by proving the maxima set conditions and then the minima set conditions. In both proofs, the argument will proceed by ruling out all the other possibilities and give the conclusion that the optima can only be attained on the theorem boundaries.

Before developing the proof it is useful to exhibit the optimization conditions verified at maxima and minima points at a 3 variables function.

First order conditions As for the first order conditions in optimization it is known that:

$$\frac{\partial H}{\partial x} = \frac{\partial H}{\partial y} = \frac{\partial H}{\partial \tau} = 0. \tag{2.8}$$

Second order conditions Here the conditions are more specific, with differences for maxima and minima. Being known that the current optimization applies to a set of points, as opposed to a single point, each of these will be represented by a negative semidefinite matrix for a maxima set and a positive semidefinite matrix in the minima case, as opposed to the non semidefinite cases for individual points.

So for a given size 3 square Hessian matrix aggregating the second order derivatives, and $\triangle_k$ representing the minor of order k: the Maxima will have its Negative semidefinite matrix with $\triangle_1 \leq 0$, $\triangle_2 \geq 0$, $\triangle_3 \leq 0$, and the Minima by its turn will be represented by a Positive Semidefinite matrix with $\triangle_k \geq 0$ for $k = 1, 2, 3$.

A - Maxima

A1 - Internal Point

Defining $(\tau^{'}, x^{'}, y^{'})$ as the internal maxima and $H^1(\tau^{'}, x^{'}, y^{'})$ as the correspondent value in H, by the definition of maxima it follows that $H^1(\tau^{'}, x^{'}, y^{'}) \geq H(\tau, g(\tau, y), y)$, that is, the maxima points must represent a greater or equal value than the boundary values.

As stated before $H(\tau, g(\tau, y), y) = F(\tau, y) > 0$, implying $H^1(\tau^{'}, x^{'}, y^{'}) > 0$

Assuming the simplified notation $O \equiv \frac{\partial^2 h}{\partial x^2}$, $P \equiv \frac{\partial^2 h}{\partial x \partial y}$, $Q \equiv \frac{\partial^2 h}{\partial y^2}$ and by substituting the first order conditions in the Heston PDE, the following form arises for the price H.

$$\frac{1}{2} y x^2 O + \rho \sigma y x P + \frac{1}{2} v^2 y Q = rH. \tag{2.9}$$

Given that the maxima Hessian matrix will be negative semidefinite, being defined as $\begin{bmatrix} O & P & \frac{\partial^2 H}{\partial x \partial \tau} \\ P & Q & \frac{\partial^2 H}{\partial y \partial \tau} \\ \frac{\partial^2 H}{\partial x \partial \tau} & \frac{\partial^2 H}{\partial y \partial \tau} & \frac{\partial^2 H}{\partial \tau^2} \end{bmatrix}$, and $O \leq 0$ due to the first two maxima conditions it must follow that $OQ - P^2 \geq 0$.

For the $O \neq 0$ case the Heston expression can be rearranged in the following fashion:

$$\begin{aligned} &\frac{1}{2} y x^2 O + \rho v y x P + \frac{1}{2} v^2 y Q = \\ &\frac{1}{2} y O \Big(x^2 + \frac{2 \rho v y x P}{O} + \frac{v^2 Q}{O} \Big) = \\ &\frac{1}{2} y O \Big(x^2 + \frac{2 \rho v x P}{O} + \frac{v^2 y Q O}{O^2} + \frac{P^2 \rho^2 v^2}{O^2} - \frac{P^2 \rho^2 v^2}{O^2} \Big) = \\ &\frac{1}{2} y O \Big[\Big(x + \frac{P \rho v}{O} \Big)^2 + \Big(\frac{OQ - P^2 \rho^2}{O^2} \Big) v^2 \Big] \end{aligned} \tag{2.10}$$

Given that $\rho \leq 1$ then, $OQ - P^2\rho^2 > OQ - P^2 > 0$ and $O < 0$, so all the elements inside the brackets will be positive and multiplied by a negative O, resulting in the right hand side of the Heston PDE verifying $rH < 0$ resulting in a contradiction with $H^1(\tau^{'}, x^{'}, y^{'}) > 0$ given that $r > 0$, and so the maxima cannot be reached under these conditions.

The case where $O = 0$ will imply that $P = 0$ and $rH = \frac{1}{2} Q v^2 y$. It will also be true that $\triangle_3 = -\frac{\partial^2 H}{\partial x \partial \tau} \frac{\partial^2 H}{\partial x \partial \tau} Q$, so our maxima set can only be attained if $\triangle_3 \leq 0$, which would imply $Q \geq 0$, and if in the Hessian matrix the order of x and y is switched it follows from Δ_1 that $Q \geq 0$, from Δ_2 $P = 0$ and from Δ_3 $Q \leq 0$ which implies $Q = 0$, and hence contradict $H^1(\tau^{'}, x^{'}, y^{'}) > 0$.

In summary these conditions lead to the conclusion that the maxima cannot be attained in the interior emerges.

A2 - Boundary $\hat{T}$

Defining the set $(\hat{T}, x^{'}, y^{'})$, it must be verified again that $H(\hat{T}, x^{'}, y^{'}) \geq max_{\tau,y} F(\tau, y) > 0$. For the first order conditions now $\frac{\partial H}{\partial \tau} \geq 0$, as the maxima are attained in a τ border, while

the other conditions subsist, so now by substituting in the Heston PDE

$$rH = \frac{1}{2}yx^2O + \rho vyxP + \frac{1}{2}v^2yQ - \frac{\partial H}{\partial \tau} \tag{2.11}$$

and by performing a very similar manipulation to the one in **A1 - Interior Point** it follows that

$$H = \frac{1}{r}\Big(\frac{1}{2}yO\Big[\Big(x + \frac{P\rho v}{O}\Big)^2 + \Big(\frac{OQ - P^2\rho^2}{O^2}\Big)v^2\Big]\Big) - \frac{1}{r}\frac{\partial H}{\partial \tau}. \tag{2.12}$$

Again, the conditions for the local maxima are $O \leq 0$ and $OQ - P^2 \geq 0$. In the $O < 0$ case given that $\frac{\partial H}{\partial \tau} \geq 0$ it will imply $-\frac{1}{r}\frac{\partial H}{\partial \tau} \leq 0$, and by the same arguments as before the contradiction of $H < 0$ will be achieved again. In the $O = 0$ case by the previous arguments hold again and give $H = \frac{1}{2r}Qv^2y - \frac{1}{r}\frac{\partial H}{\partial \tau}$, which will not validate the maxima, assuming the conclusion from **A1 - Interior Point**, leads to the $H(\hat{T}, x^{'}, y^{'}) < 0$ contradiction. So the maxima cannot be achieved at the $r = \hat{T}$ boundary.

A3 - Boundary $y = 0$

In this case, the specific PDE for the $y = 0$ will hold, and in the first order conditions it will result in $\frac{\partial H}{\partial y} \leq 0$, as in order to have maxima at the $y = 0$ border the variation in H will have to be negative as the values of y increases. So by substituting first order conditions in the equation the following will be obtained:

$$\kappa\theta\frac{\partial H}{\partial y}\frac{1}{r} = H \tag{2.13}$$

Due to $\frac{\partial H}{\partial y} \leq 0$ it will emerge that $H \leq 0$, once again preventing maxima due to $F(\tau, y) > 0$.

A4 - Boundary $y = \hat{Y}$

Considering the case with a sizeable amount of volatility, that is, as $y \to \infty$, or the set $(\tau^{'}, x^{'}, \hat{Y})$. The first order conditions now will result in $\frac{\partial H}{\partial y} \geq 0$, and for the sake of convenience it will be required that $\hat{Y} > \max[(\frac{\lambda v}{2\kappa})^2, \theta]$, as this constrain will assure that the term that multiplies by $\frac{\partial H}{\partial y}$ will follow the restriction:

$$\kappa(\theta - y) - \sqrt{y}\lambda v < 0. \tag{2.14}$$

As for the proof of the condition above, in the case $\hat{Y} > (\frac{\lambda v}{2\kappa})^2 \geq \theta$ can be written in the following manner where the condition will be assured given the positivity of the parameters:

$$\kappa\Big(\theta - \Big(\frac{\lambda v}{2\kappa}\Big)^{2+}\Big) - \lambda v\Big(\frac{\lambda v}{2\kappa}\Big)^{+} < 0. \tag{2.15}$$

The first component multiplied by κ following the restriction, will be negative, while second is a square product of λv divided by positive 2κ multiplied by -1 and so negative. with both terms negative the < 0 condition is fulfilled, even if $\lambda = 0$ due to $\hat{Y} > (\frac{\lambda v}{2\kappa})^2$.

For the condition $\hat{Y} > \theta \geq (\frac{\lambda v}{2\kappa})^2$ written as

$$\kappa(\theta - \theta^{+}) - v\lambda\sqrt{\theta^{+}} < 0 \tag{2.16}$$

Clearly satisfies the condition, which the positivity of the parameters and similar arguments as to those above, even when $\lambda = 0$, where $\hat{Y} > \theta$ proves advantageous.

Although the above conditions demand assuming the parameters, for $\theta < \hat{T}$ it is easy to fulfil, as the maximum volatility should be greater than its long term level, the second will dependent on the parameters chosen, although with the consideration that λ tends to be assumed 0 on many occasions.

So by replacing the first order conditions in the Heston PDE

$$H = \frac{1}{r}\Big(\frac{1}{2}yO\Big[\Big(x + \frac{P\rho v}{O}\Big)^2 + \Big(\frac{OQ - P^2\rho^2}{O^2}\Big)v^2\Big]\Big) + \frac{1}{r}[\kappa(\theta - y) - \sqrt{y}\Lambda v]\frac{\partial H}{\partial y}. \tag{2.17}$$

With the component $[\kappa(\theta - y) - \sqrt{y}\Lambda v]$ being assured as negative and $\frac{\partial H}{\partial y}$ positive the previous arguments will hold, and once again $H < 0$ will occur, resulting in the contradiction with having a maxima set as $y \to \infty$.

A5 - Boundary $\tau = 0$

At the set $(0, x, y)$, following the first condition there is $H(0, x, y) = 0$, thus contradicting $F(\tau, y) > 0$. So it can be concluded with all the other possible sets being rejected it can be concluded that the maxima boundary is achieved at $(\tau, g(\tau, y), y)$.

B - Minima

B1 - Internal Point

As for the Minima, not developed in CM(2011), defining $(r^{'}, x^{'}, y^{'})$ as the internal minima

set, and $H^1(r^{'}, x^{'}, y^{'})$ as its value. As it is known $H(0, x, y) = 0$ and as the option price must be non-negative a given internal minima will respect $H^1(r^{'}, x^{'}, y^{'}) = 0$.

Substituting the internal maxima conditions once again the known expression is obtained and transformed in the usual matter:

$$\frac{1}{2}yx^2O + \rho vyxP + \frac{1}{2}v^2yQ = rH \tag{2.18}$$

$$\frac{1}{2}yO\Big[\Big(x + \frac{P\rho v}{O}\Big)^2 + \Big(\frac{OQ - P^2\rho^2}{O^2}\Big)v^2\Big] = rH. \tag{2.19}$$

Following the maxima set condition, if $O > 0$ then $OQ - P^2 \geq 0$ all the elements of the above equation will be composed by positive numbers and zeros, resulting in a $rH > 0$ raising an inconsistency with $H = 0$.

On the other side if $O = 0$ then for $\triangle_2 = OQ - P^2 \geq 0$ will imply $P = 0$, and in order to have $\triangle_3 \geq 0$ it would require $Q \leq 0$, and similarly to at **A1 - Internal point**, by switching x and y $Q \leq 0$ and $Q \geq 0$, so $Q = 0$ which would contemplate $rH = 0$, an impossibility and so making it impossible to find minima at the interior.

B2 - Boundary $\tau = \hat{T}$

Once again with $0 = \min_{\tau,y} F(\tau, y) = H(\hat{T}, x^{'}, y^{'})$, and having the specific first order condition $\frac{\partial h}{\partial \tau} \leq 0$, that is, if τ is increasing H is decreasing to reach the minima set, while applying the standard conditions for x and y, through substitution in the usual transformed Heston PDE:

$$rH = \frac{1}{2}yO\Big[\Big(x + \frac{P\rho v}{O}\Big)^2 + \Big(\frac{OQ - P^2\rho^2}{O^2}\Big)v^2\Big] - \frac{1}{r}\frac{\partial H}{\partial \tau}. \tag{2.20}$$

Due to the last term being the product of two negative components it will be positive, and summed with the equation from B1 it can contradict with $H^1(r^{'}, x^{'}, y^{'}) = 0$, making it impossible to have minima at $\tau = T$.

B3 - Boundary $y = 0$

As in the maxima case, the condition at $y = 0$, with the only difference now that $\frac{\partial H}{\partial y} \geq 0$, as H will increase departing from the minima, so now through substitution in the condition $\kappa\theta\frac{\partial H}{\partial y}\frac{1}{r} = H$ will arise again, although this time $H \geq 0$, which does not guarantee the minima

to be zero, going for an additional a contradiction.

B4 - Boundary $y = \hat{Y}$

Again, as $y \to \infty$, the set $(\tau^{'}, x^{'}, \hat{Y})$, although now for the minima $\frac{\partial H}{\partial h} \leq 0$, the same expression as in the maxima for this border will appear, with the difference that the last term will be the product of two negative terms, with same condition $\hat{Y} > \max[(\frac{\lambda v}{2\kappa})^2, \theta]$, therefore positive, which is summed with the remaining positive part as seen previously, arising the contradiction and invalidating maxima at the $\hat{Y}$ boundary.

B5 - Boundary $(\tau, g(\tau, y), y)$

Given that $H(\tau, g(\tau, y), y) = F(\tau, y) > 0$, this leading to an obvious inconsistency.

Again, all the other possible sets are rejected, and the minima needs to be achieved and $\tau = 0$ ■

2.2.2. Proof of Proposition 3.1

Assuming the existence of 2 solutions, h_1 and h_2, and the solutions being solved by the equation $h^{'} = h_1 - h_2$. At both h_1 and h_2 the generated solution set for the maxima will achieved at $(\tau, g(\tau, y), y)$ due to the base theorem, being represented by the same value $F(\tau, y)$, which will lead to $h^{'} = 0$ at $g(\tau, y)$, and given that it is the maxima set due to *Proposition 0* $h^{'} = 0$ will be present at the whole set implying $h_1 = h_2$. ■

2.2.3. Proof of Proposition 3.2

Let $\hat{C}^0 = \{(\tau, x, y) \in (0, \hat{T}) \times \mathbb{R}^2_+ | x > b^0(\tau, y)\}$ and $\hat{C}^{b^*} = \{(\tau, x, y) \in (0, \hat{T}) \times \mathbb{R}^2_+ | x > b(\tau, y)\}$. In the region in between, $\hat{C}^0 - \hat{C}^{b^*}$, it is optimal to exercise, but the dictated exercise policy chooses to sub-optimally hold, this is, in this in-between region $p^0 < p^{b^*} = (K - x)^+$. On the other side, over b^0 it will be that $p^0 = (K - x)^+$, and also by Base Theorem the non-negative maxima will be achieved on b^0. So it will emerge that $p^0 = K - x$ and recalling that $p^0 < K - x$ in the $\hat{C}^0 - \hat{C}^{b^*}$ region, which will imply that as there is a price of x increase the price of the put for policy b^0, p^0 does not decrease in the same magnitude, which translates into $\frac{\partial p^0}{\partial x}|_{(\tau, b^0(\tau, y)^+, y)} < -1$. ■

2.2.4. Theorem 3.1

Using for the following notation in the proof: $\frac{\partial p^n}{\partial x}|_{(\tau, b^n(\tau, y), y)} = p^n_x$.

Since $p_x^n(\tau, b_n(\tau,y)^y, y) < -1$ and $lim_{x\to\infty}\ p_x^n(\tau,x,y) = 0$, b^{n+1} exists due to the continuity of p_x^n in $\hat{C}^n$, b^{n+1} exists, defining $\hat{C}^n = \{(\tau,x,y) \in (0,\hat{T}) \times \mathbb{R}_+^2 | x > b^n(\tau,y)\}$.

From the definition of b^{n+1}, (which respects $b^{n+1} > b^n$), for all $x \in (b^n(\tau,y), b^{n+1}(\tau,y))$, τ and y, it is verified $p_x^n(\tau,x,y) < -1$, or in other words, this regions of x is obtained by verifying where the underlying price is decreased, the put price increases in a lesser magnitude. Given that in the region $x = b^i(\tau,y)$ with $i \in \{n, n+1\}$ it will imply that for the same applied boundary the difference in price at each boundary is less than the difference in boundaries for a put:

$$\begin{aligned}
&p^n(\tau, b^{n+1}(\tau,y), y) - p^n(\tau, b^n(\tau,y), y) < b(\tau,y)^n - b(\tau,y)^{n+1} \\
&p^n(\tau, b^{n+1}(\tau,y), y) < p^n(\tau, b^n(\tau,y), y) + b(\tau,y)^n - b(\tau,y)^{n+1} \\
&= (K - b(\tau,y)^n) + b(\tau,y)^n - b(\tau,y)^{n+1} \\
&= K - b(\tau,y)^{n+1} \\
&= p^{n+1}(\tau, b^{n+1}(\tau,y), y),
\end{aligned} \tag{2.21}$$

which translates into $p^{n+1} > p^n$ when using the boundary b^{n+1}.

Now the difference $\hat{p} = p^{n+1} - p^n$ solves the following conditions:

$$\begin{aligned}
&Lp = 0 \quad in \quad \hat{C}^{n+1}, \\
&\hat{p}(0,x,y) = 0, \\
&\hat{p}(\tau, b^{n+1}(\tau,y), y) > 0, \\
&\lim_{x\to\infty} \hat{p}(\tau,x,y) = 0, \\
&\lim_{y\to\infty} \hat{p}(\tau,x,y) = 0, \\
&A\hat{p} = 0.
\end{aligned} \tag{2.22}$$

Using the result from the Base theorem, it is known that $\hat{p}$ attains its maxima on b^{n+1} and its minima of 0 on the boundary $(0,x,y)$ for $(x,y) \in (b^{n+1}, \infty) \times \mathbb{R}_+$. Given its positive maxima set we concluded $\hat{p} > 0$ in $\hat{C}^{n+1}$, or given how it is defined, $p^{n+1} > p^n$.

Regarding the second part of the Theorem, going from $p_x^{n+1} = p_x^n + \hat{p_x}$ and knowing by definition $p_x^n(\tau, b^{n+1}(\tau,y), y) = -1$ (the way one finds to discover b^{n+1} value), it will be sufficient to show that $\hat{p}_x^n(\tau, b^{n+1}(\tau,y), y) < 0$, that is, the difference between the two

derivatives dependent on two exercise policies will be negative, therefore summing -1 to a negative value.

By assuming that $\hat{p}_x^n(\tau, b^{n+1}(\tau, y), y) \geq 0$, since $\lim_{x\to\infty} \hat{p_x}(\tau, x, y) = 0$, the assumption would imply the existence of maxima in C^{n+1}, as the put price increases or remains stable until x reaches a first order condition, which contradicts the Base Theorem, that demands the maxima not to be obtained in the Continuation region. Due to the negative variation in $\hat{p}$ it will emerge that $p_x^{n+1}(\tau, b^{n+1}(\tau, y)+, y) < -1$. ■

2.3. Illustration of the Procedure

Through an example the Transformation procedure will be exemplified, showing the underlying dynamics. Using the same parameters as in CM(2011):

$\hat{T}$ - Time to expiry maximum	0.250
$\hat{X}$ - Spot maximum	20
$\hat{Y}$ - Volatility maximum	2
K - Strike	10

Table 2.1.: Base parameters

r - Interest rate	10%
κ - Volatility speed of reversion	5
θ - Long term variance	0.16
σ - Volatility of variance	0.5
ρ - Spot/Volatility correlation	0.1

Table 2.2.: Model parameters

l - Time partition	4000
m - Spot partition	80
n - Volatility partition	80

Table 2.3.: Partition parameters

The initial guess of the initial boundary is set to $b^0 = 1$ as in Chockalingam and Muthuraman (2011).

To stop the iterations, CM(2011) set a level of convergence for the succession of iterations to be executed between the boundaries, that is, for each new iteration b^{n+1} it should respect $b^{n+1} - b^n < \epsilon_b$, or alternatively it can be set for the price function as $p^{n+1} - p^n < \epsilon_p$. For

the transformation procedure in this document the tolerance is set in terms of the boundary, with $\sum b^{n+1} - b^n < \epsilon_b$.

In this section, to assure precision the tolerance is going to be set at $\epsilon_b = 0$, meaning that $b^{n+1} = b^n$ is the condition for the iteration to stop, carrying the Procedure until the condition $p^n < (K - x)^+$ is no longer verified.

The first policy of b^0 eventually is iterated and improved to b^n at $\tau = 0.250$.

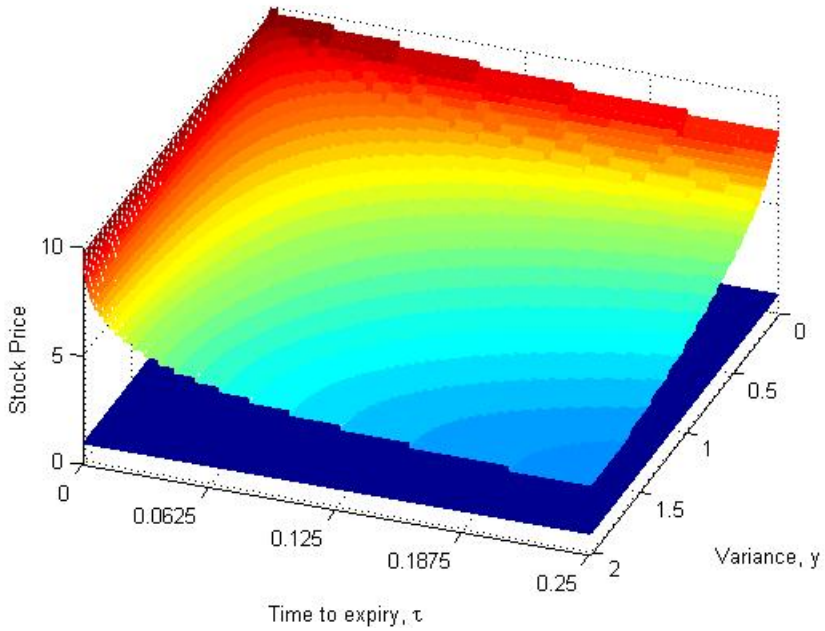

Figure 2.1.: Initial and Final exercise policies

As shown in figure 2.1 b^0 ends in b^n

The progress occurs through several iterations, as below:

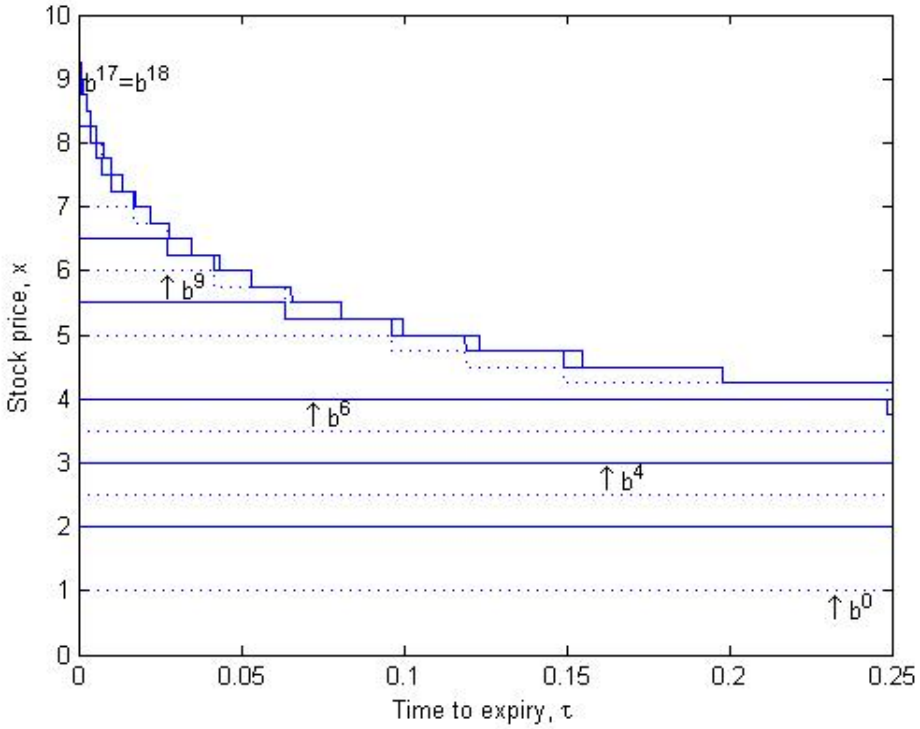

Figure 2.2.: Improvement sequence

As it is clear in the figure above, with uneven boundary numbers represented by dotted lines, while the remainder are in solid lines, the policy starting at $b^0 = 1$ gradually improves until it converges to $b^{17} = b^{18}$. As the improvement policies are calculated separately for each τ, at different times to expiry there are different number of iterations required, and so in the figure when the iterations were below the maximum 18 the extra iterations do not affect the boundary, i.e., if at a given τ the iterations end at b^{13} it will be that $b^{13} = b^{14} = ... = b^{18}$. It is also observable that the manner to iterate is different than the one observed in the illustration of CM(2011), this theme is discussed further below in this section.

To observe in greater detail how the derivatives work in the procedure at the cut $y = 1$ in the $\tau = 0.0125$ period the policy improvement occurs as the sequence below shows.

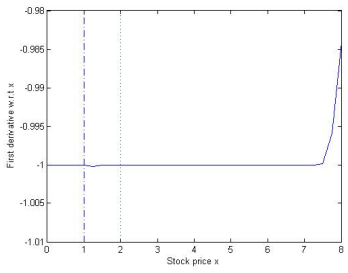

(a) Improvement following derivatives

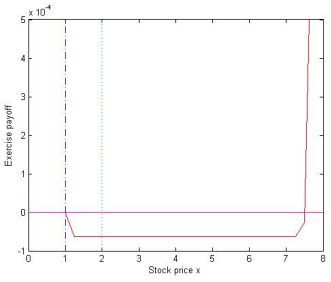

(b) Difference to the exercise barrier

Figure 2.3.: b^0 result

The first dashed and dotted line represents the initial boundary, while the dotted line to the right is the last value where $\frac{\partial p}{\partial x} \leq -1$ is verified, where the following boundary will advance to. Although the condition to find the next boundary states to progress to value a x_1 that verifies $\frac{\partial p}{\partial x} < -1$, it is clear that if the following value x_2 verifies $\frac{\partial p}{\partial x} = -1$, as soon as x_1 is included in the stoppig region x_2 will verify $\frac{\partial p}{\partial x} < -1$, making it faster to iterate by seeking $\frac{\partial p}{\partial x} \leq -1$ without loosing precision in the method.

So by further progressing the method's iterations in the described manner:

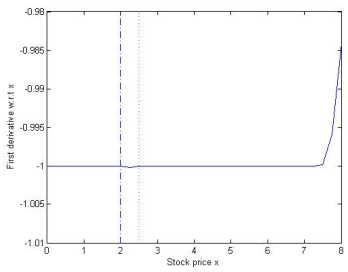

(a) Improvement following the derivative

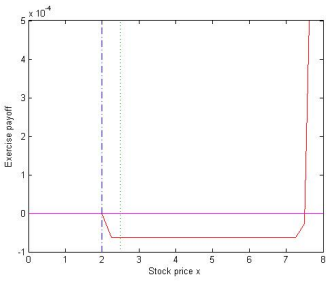

(b) Difference to the exercise barrier

Figure 2.4.: b^1 result

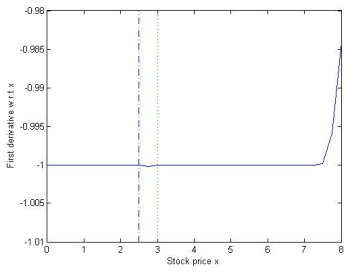

(a) Improvement following the derivative

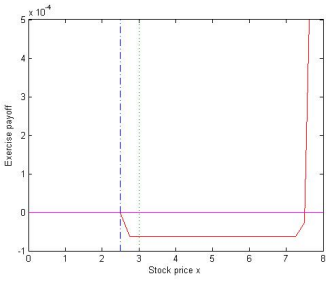

(b) Difference to the exercise barrier

Figure 2.5.: b^2 result

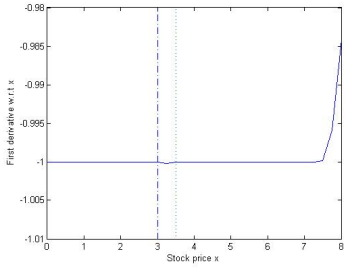

(a) Improvement following the derivative

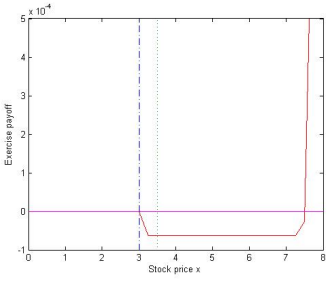

(b) Difference to the exercise barrier

Figure 2.6.: b^3 result

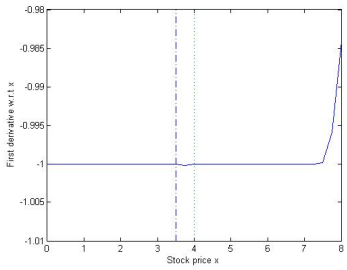

(a) Improvement following the derivative

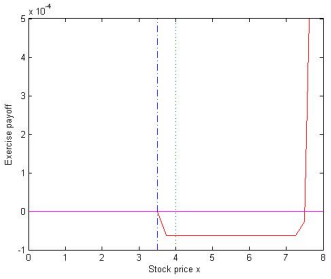

(b) Difference to the exercise barrier

Figure 2.7.: b^4 result

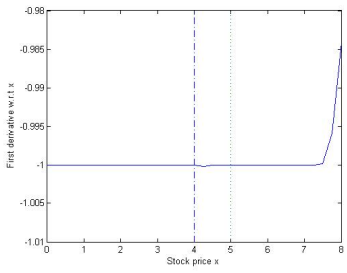

(a) Improvement following the derivative

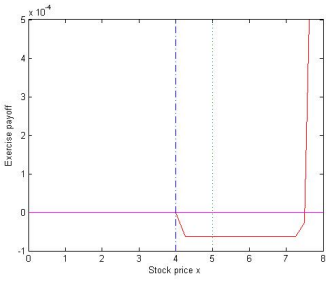

(b) Difference to the exercise barrier

Figure 2.8.: b^5 result

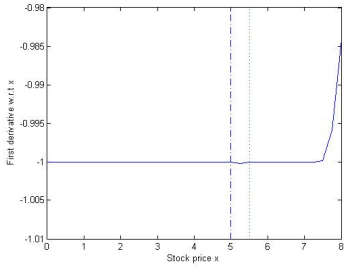

(a) Improvement following the derivative

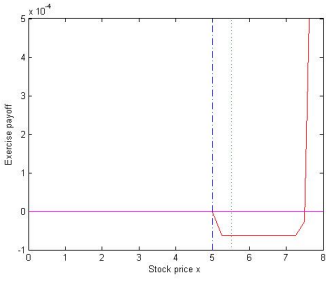

(b) Difference to the exercise barrier

Figure 2.9.: b^6 result

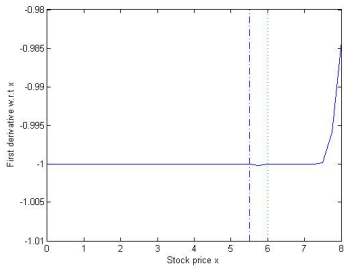

(a) Improvement following the derivative

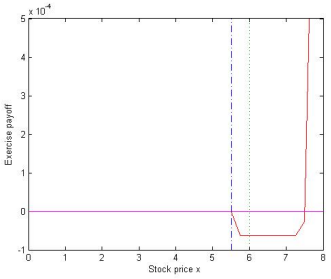

(b) Difference to the exercise barrier

Figure 2.10.: b^7 result

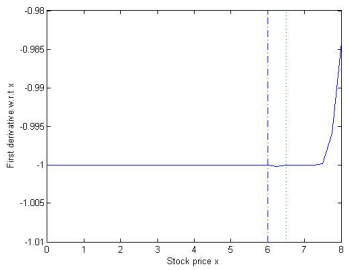

(a) Improvement following the derivative

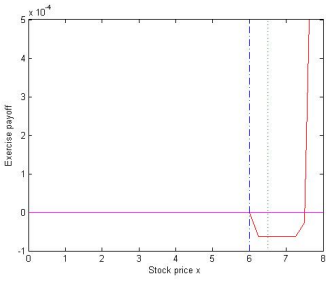

(b) Difference to the exercise barrier

Figure 2.11.: b^8 result

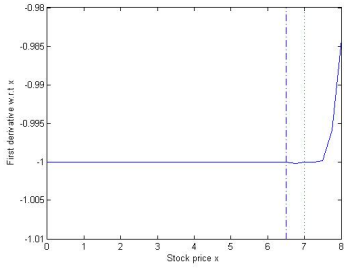

(a) Improvement following the derivative

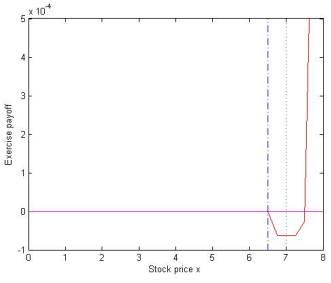

(b) Difference to the exercise barrier

Figure 2.12.: b^9 result

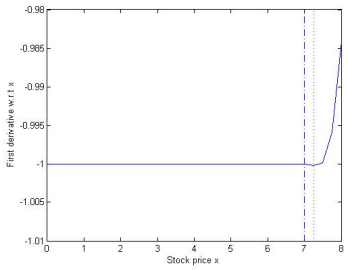

(a) Improvement following the derivative

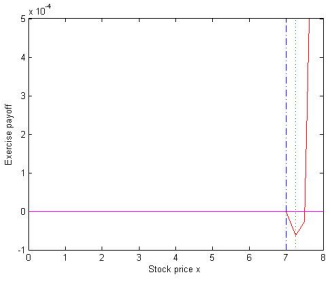

(b) Difference to the exercise barrier

Figure 2.13.: b^{10} result

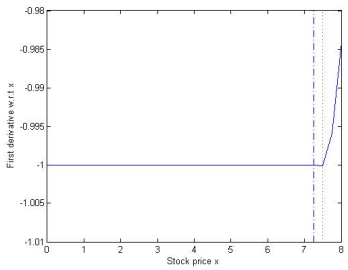

(a) Improvement following the derivative

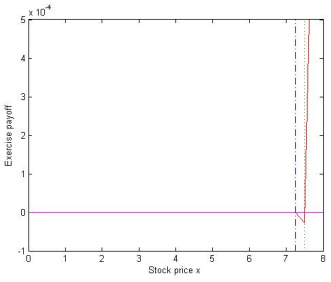

(b) Difference to the exercise barrier

Figure 2.14.: b^{11} result

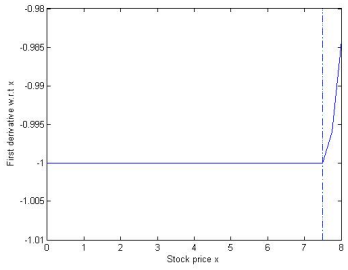

(a) Improvement following the derivative

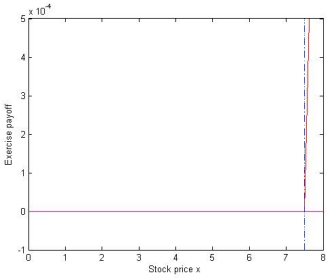

(b) Difference to the exercise barrier

Figure 2.15.: b^{12} result

As the procedure exhausts the $p < K - x$ condition the iterations do not find more values to proceed, and so $b^{12} = b^{13}$, leading to the end of the process and the start of calculations in the following τ. The difference in the number of iterations for the whole procedure and the presented cut is justified by the different progress for various volatility vectors.

In CM(2011) the illustration of the process displays a slightly different disposition both in the improvement sequence and in the derivate illustration, for instance, as the iterations progress values to the right of the new boundary display changes, while overall there are less iterations registered. A fair explanation seems to rely on how the iterations are computed, in contraposition to this thesis that calculates all the iterations for a given τ and then progress, in the illustration CM(2011) likely compute from a given b value p for the whole τ set, and only iterating after $\hat{T}$ is reached. This kind of iteration shows a more interesting illustration despite slower computational performance, as each iteration requires recalculating

all the continuation region. In the following graphs an illustration with this methodology is presented, while for the rest of the thesis the method of calculating all the iterations for a given τ and only then proceeding will be used.

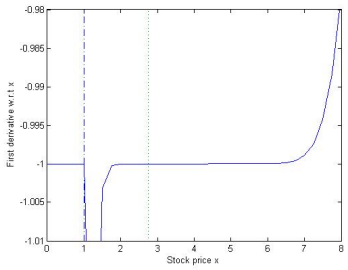

(a) Improvement following the derivative

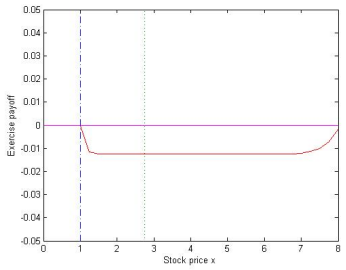

(b) Difference to the exercise barrier

Figure 2.16.: b^0 result

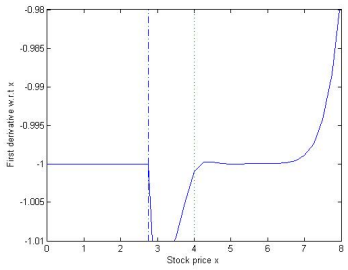

(a) Improvement following the derivative

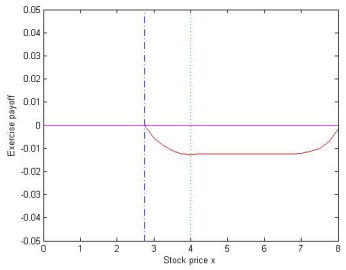

(b) Difference to the exercise barrier

Figure 2.17.: b^1 result

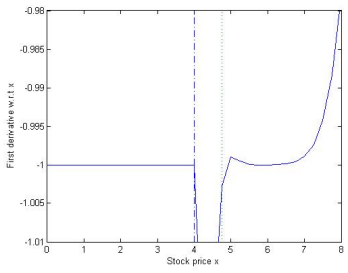

(a) Improvement following the derivative

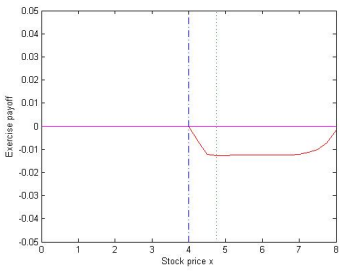

(b) Difference to the exercise barrier

Figure 2.18.: b^2 result

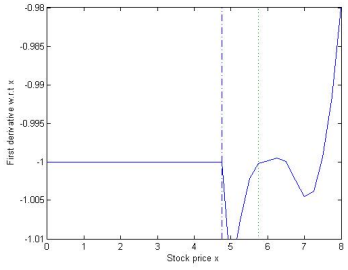

(a) Improvement following the derivative

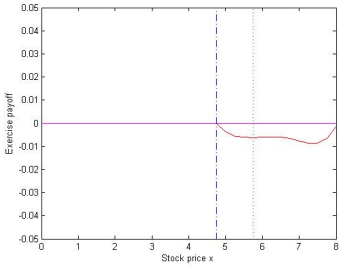

(b) Difference to the exercise barrier

Figure 2.19.: b^3 result

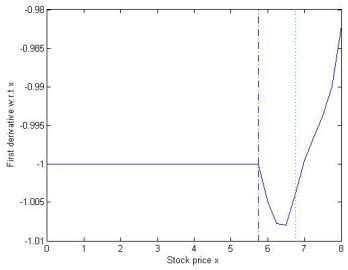

(a) Improvement following the derivative

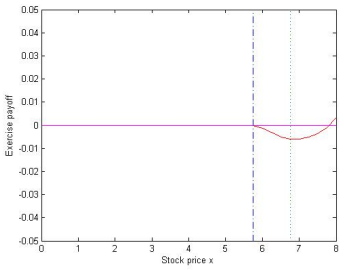

(b) Difference to the exercise barrier

Figure 2.20.: b^4 result

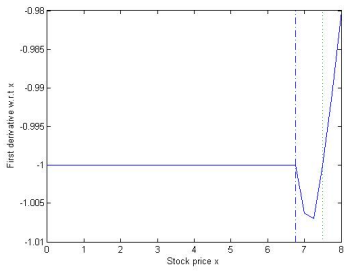

(a) Improvement following the derivative

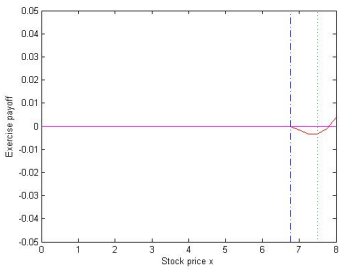

(b) Difference to the exercise barrier

Figure 2.21.: b^5 result

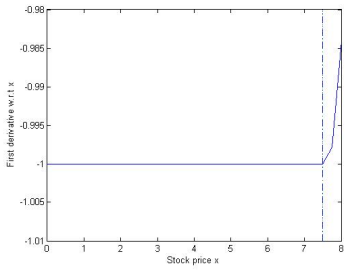

(a) Improvement following the derivative

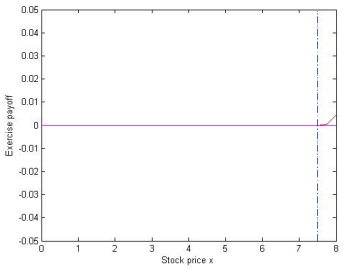

(b) Difference to the exercise barrier

Figure 2.22.: b^6 result

As observed, the process is executed with less iterations (although more computational demanding), while the value at spot prices at the right of the barrier increase along the process. As the iterations also change the values at lower τ sections, reaching the same barrier in the end with very similar values for the other spot price.

2.4. Results and benchmarking

Using the method for different spot and volatility levels the following results arise, with spot price on the vertical axis and volatility on the horizontal, for both the baseline case and changing the dividend yield to 5%, which increases the prices as expected.

		0.25	0.5	0.75	1	1,25	1.5	1.75
$q = 0$	4	2.0741	2.231	2.3806	2.5186	2.6463	2.7655	2.8777
	8	0.247	0.4625	0.6569	0.834	0.9979	1.152	1.2983
$q = 5\%$	4	2.1091	2.2704	2.4205	2.5582	2.6854	2.804	2.9156
	8	0.2684	0.4889	0.6859	0.8644	1.0293	1.184	1.3308

Table 2.4.: Results table

In order to test the accuracy of the transformation result, it will be compared to the First Difference method that as calculating the price through the PDE verifies for each τ, x, y the hold or exercise method with the criteria $p(\tau, y, x) = \max[p(\tau, x, y); K - x]$.

Using the same parameters used in the stability testing at $\hat{T} = 0.250$ it is verified that, when setting tolerance between iterations to 0, the results are the same, as one would expect.

However, if the tolerance level is changed the results can be different. In CM(2011) the tolerance value is only mentioned to have a small value. In this thesis this will be formalized, setting a tolerance level as to keep iterating at $\sum b^{n+1} - b^n > (n+1) \times \delta_s \times \gamma$, that is setting the *gamma* parameter to be multiplied by the number of points the exercise-boundary engulfs and by how much each spot value it progresses.

And choosing now $\gamma = 1$, that is, the procedure stops for a given τ when on average the new boundary progress less than a grid point per volatility vector.

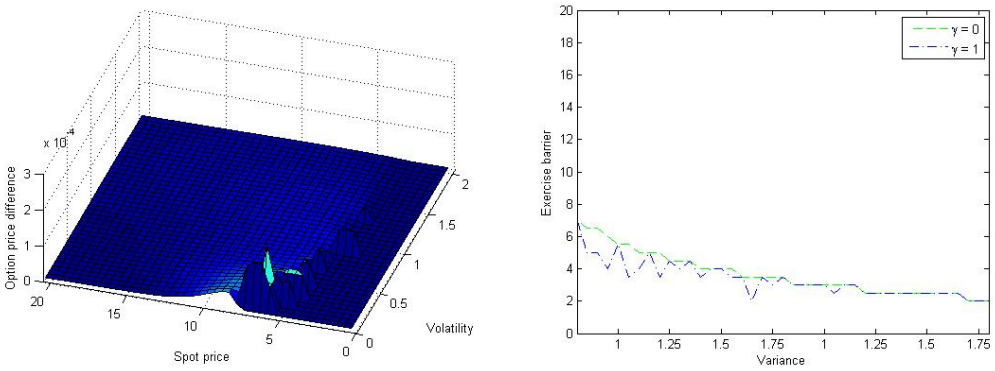

(a) Difference to benchmark

(b) Boundaries

Figure 2.23.: Comparison to the benchmark at $\gamma = 1$

Figure 2.23 reflects differences in the prices generated by the two methods at $\hat{T}$, while the boundary it set lower in many points and shows and erratic behaviour, and so setting the γ parameter different to zero can misshape the results. This phenomenon and its consequences

on method performance shall be further studied in the last chapter.

3. Parametrization insights

3.1. Stochastic volatility

The inclusion of stochastic volatility allows the improvement over the constant volatility in Black and Scholes (1973). The constant volatility setting can replicated by the Heston PDE from (1.4) by setting to 0 the correlation, volatility of the variance process, market price of risk and setting the long term of volatility to constant value, so reaching the Black Scholes PDE:

$$\frac{1}{2}vS^2\frac{\partial^2 p}{\partial x^2} + rS\frac{\partial p}{\partial x} - rp - \frac{\partial p}{\partial \tau} = 0. \tag{3.1}$$

So by substituting the parameters properly the price of constant volatility American options can be reached with the Heston based model, allowing to study the impact of including stochastic volatility in American option modelling.

By using the Finite Differences, the difference between the constant and stochastic volatility models put prices are going to be tested, for the same volatility values until $T = 0.250$, with the stochastic model having $\theta = 0.4$ as the long term value for volatility. In addition, in the stochastic model $\rho = 0$ is set for a clearer comparison while the remaining parameters are equal to those in the stability section.

In the following graphs the difference $p(\tau, x, y) - p(\tau, x)|_y$ will be tested, with the former representing the put price under stochastic volatility and the latter the price under constant volatility, at variance y. Moreover, the graphs display in the dotted green line the stochastic volatility exercise boundary, and the solid red line the constant volatility boundary.

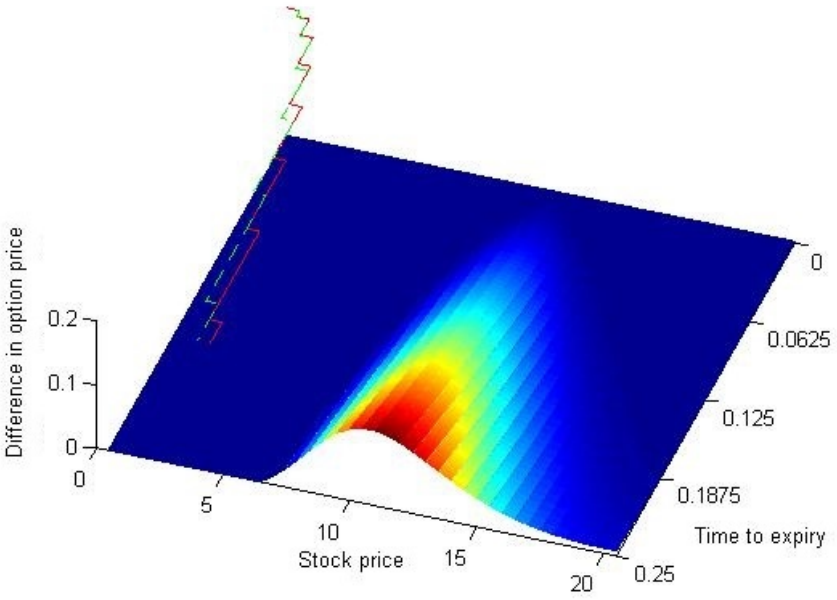

Figure 3.1.: Difference at $y = 0.2$

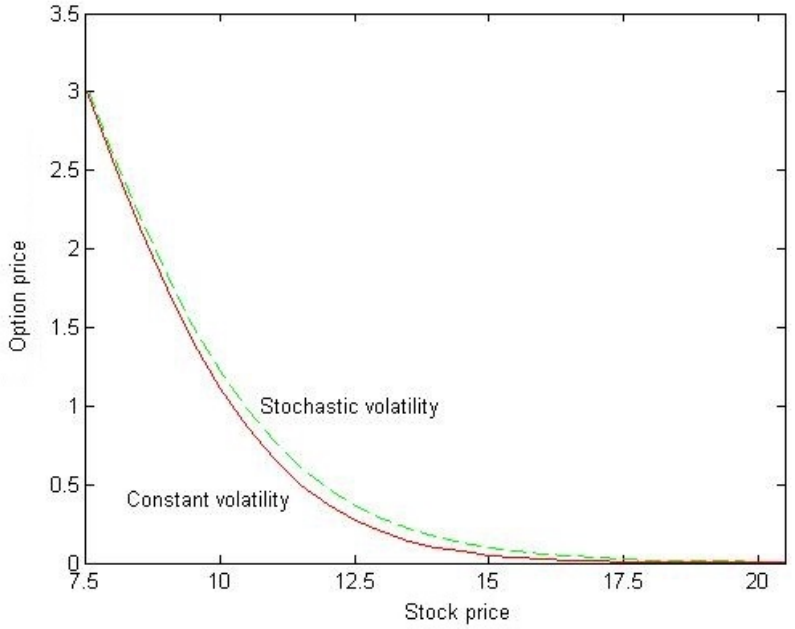

Figure 3.2.: Prices at $y = 0.2$ and $T = 0.250$

At $y = 0.2$, the difference $p(\tau, x, 0.2) - p(\tau, x)|_{0.2}$, shows that the price in the stochastic model tends to be higher, mostly around at-the-money values. This is a reflection of the tendency for the stochastic volatility to move towards the value of $\theta = 0.4$ resulting in higher values as typically higher volatility corresponds to higher prices. This price increase increases mostly near the money, where there are bigger opportunities of moving in/out-the-money. In addition, the difference is also greater for deep out-the-money options than deep in-the-money, as in the earlier volatility is needed for the price to go below the strike and the latter the option is as more chances of having been early-exercised thus no longer affected by volatility. As for the exercise boundary, it is higher for the constant volatility case, as lower option values imply the early exercise to be used for a wider range of values.

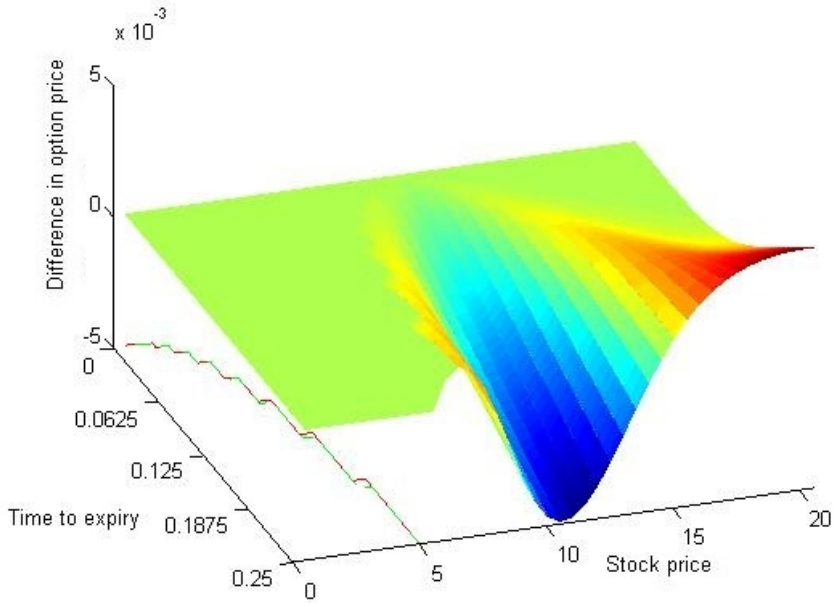

Figure 3.3.: Difference $y = 0.4$

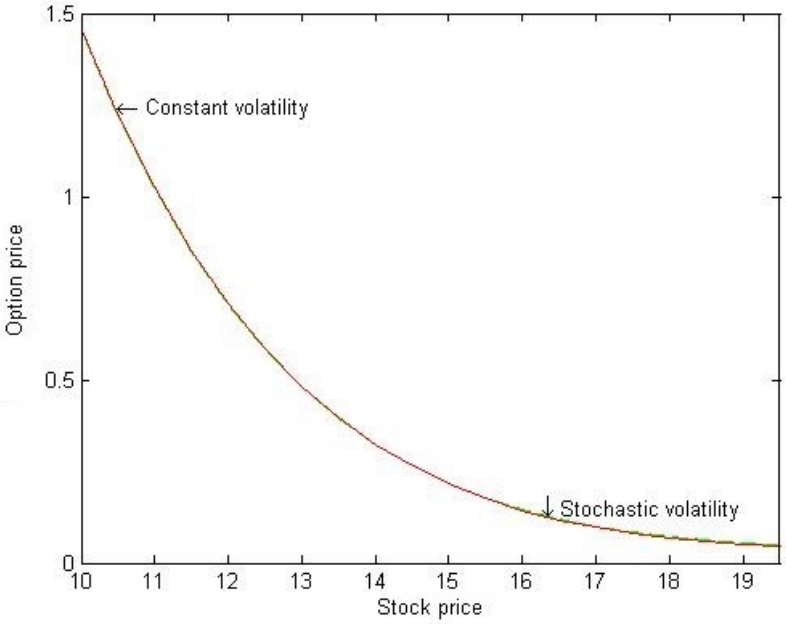

Figure 3.4.: Prices at $y = 0.4$ and $T = 0.250$

In the $y = 0.4$ case, where the stochastic model the volatility is equal to the long term average, the price difference tends to be of a much lower scale with no constant pattern, due to the two volatilities being virtually the same, and the exercise boundaries tend to be equal, given the prices' likeliness.

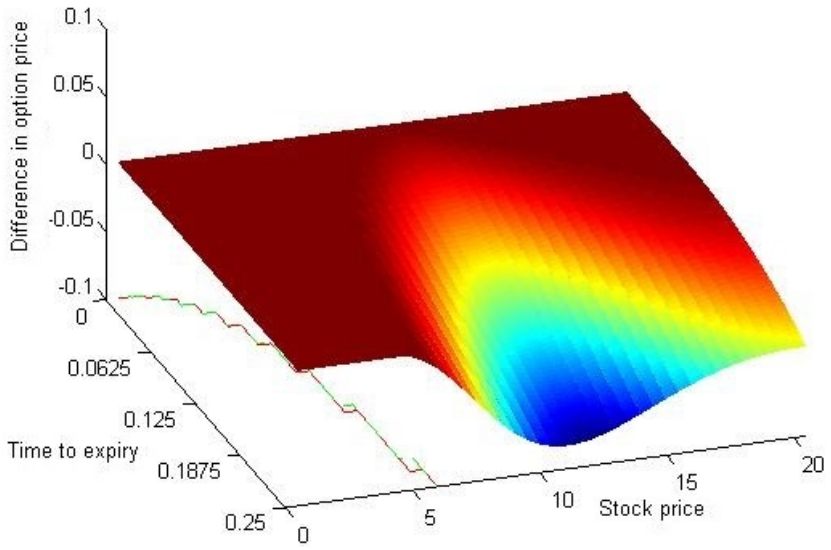

Figure 3.5.: Difference at $y = 0.6$

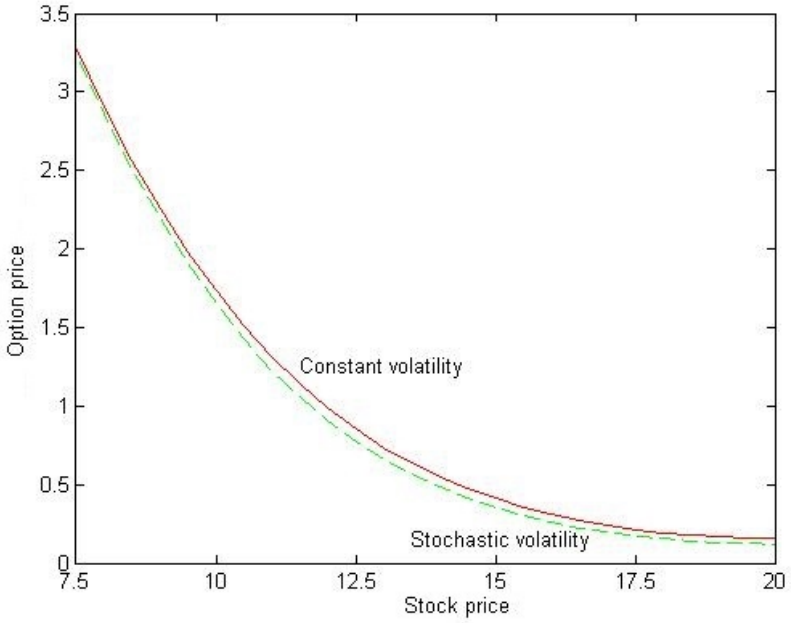

Figure 3.6.: Prices at $y = 0.6$ and $T = 0.250$

Lastly, the situation is reversed when compared to the first case, as the stochastic model starts at 0.6 and tends towards 0.4, with the constant volatility providing higher values, mostly near the money and also when deep out-the-money, while the boundary tends to be higher for the stochastic model.

Overall regarding the mispricing of options using the two different models, given investor's preference for volatility, when the instantaneous volatility is lower than long term volatility, the constant model will tend to undervalue options value, with the reverse happening then the long term volatility is lower than the instantaneous level. This difference in pricing is more pronounced for the higher stock levels in the put case, as when volatility is undervalued/overvalued, the odds of the price going below the strike are lower/higher, resulting in underpricing/overpricing, this effect is less impactful for low asset levels, as here volatility can also contribute for the option to go out-the-money, and part of the values belonging to the *stopping* region.

3.2. Correlation

The correlation between the asset price and its volatility is the main reflection of what is known as the 'leverage' effect, that states that as underlying asset prices tend to go lower, volatility tends to go higher, which is impactful in option pricing. For instance as the price of an option becomes lower, empirically it is expected that is volatility increases, leading it towards higher prices.

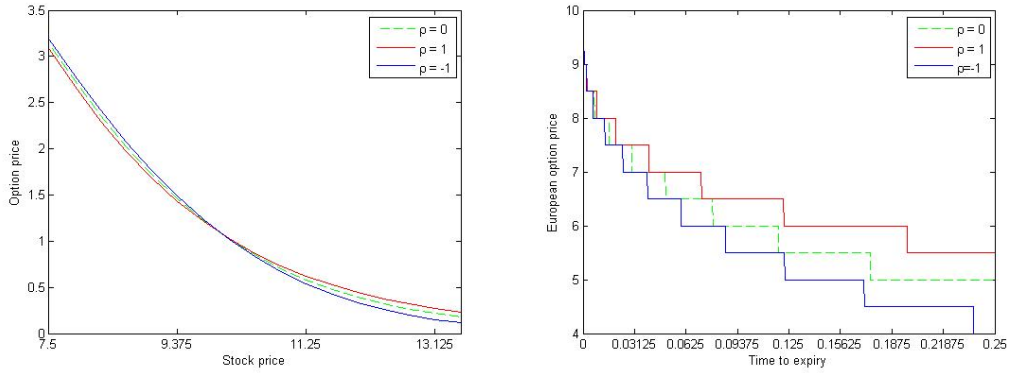

(a) Price function $y = 0.4$

(b) Exercise policies $y = 0.4$

Figure 3.7.: Price at various correlations

In the figure 3.7 above this effect is explicit for the cases of total positive and negative correlations, and in the case of null correlation. At lower values for the same spot price the lower the more negative the correlation the higher the price, while for high values the bigger the correlation the bigger the price. While for the values near at-the-money the effects tends to be null, as the correlation does not generate as much impact. This can be interpreted with the example that when the put option is out of the money it preferable to an investor to have higher volatility, which may drive the option's price to the in-the-money zone. In regards to the exercise boundary it can be noted that as correlation decreases it decreases to, as higher correlation tends to increase prices in higher values, which correspond to a big share of the *continuation* region (since lower prices tend to be in the *stopping* region, not ruled by the Heston PDE), increasing overall prices, and decreasing the incentive to early exercise.

3.3. Market price of volatility

The market price of volatility risk can be defined as the reward for holding a volatile portfolio, although usually assumed as 0 during this thesis, its inclusion in the parameters can be analysed.

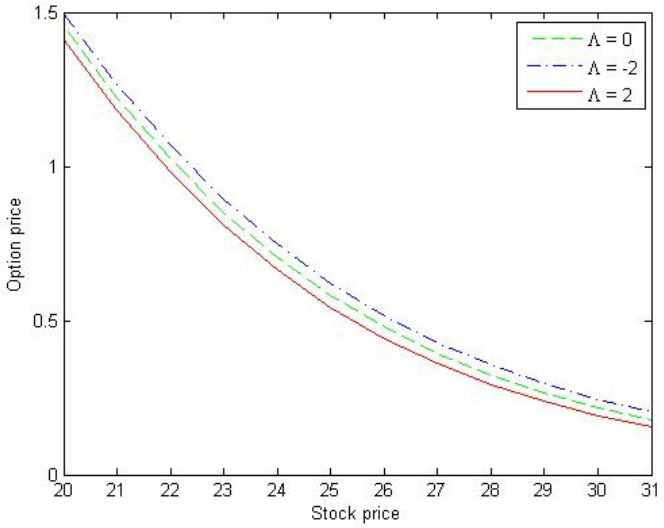

Figure 3.8.: Price at $\tau = 0.250$ $y = 0.4$

Figure 3.8 makes it clear that for the same stock price, by assuming a more negative price of volatility risk the price of the put option increases. This can be interpreted as that by considering holding volatility as undesirable, and so one should be rewarded by it. By keeping the option the investor is holding volatility risk, that is buying it, and given the more negative it is, the more the return the investor can expect its asset to be worth, on the other side, if it was considered desirable to hold risk, that is $\lambda > 0$, the investor would have to pay for it by holding a less valuable asset. Another interpretation can arise when considering the delta-hedged portfolio used to derive the Heston PDE, that considering the price of risk equal to zero, the price of the option should match the price of constructing the portfolio, but when it is priced, by having a non arbitrage argument, when the price of the volatility risk increases/decreases the price of the option decreases/increases.

4. Method efficiency and calibration

To study the computational performance, all the results in this chapter were computed in MATLAB using an Intel(R) Core i5-3337U CPU @ 1.80GHz (4 CPUs).

4.1. Partitioning

As explored in the accuracy section, by increasing the number of partitions δ_x and δ_y the precision of the results tends to be increased and the amount of individual (x, y) points is greater, but this tends to have negative effects computational burden. The increment in time required tends to be more than proportional to increase in the mesh points, mostly due to the numerical stability issues observed in the stability testing section the τ parameter must be adequate, and the proportional increase in l tends to be bigger than the one in m and n.

So with the same remainder of the parameters set as in the stability testing, below for various levels m and n, and an adequate, but not unnecessary high level τ that allows viable numerical results the computation times are compared.

Partitions in S and y	Partitions in τ	Runtime
10	10	0.007640
20	70	0.190930
30	170	1.203272
40	400	5.356751
60	800	32.930487
80	1800	105.909127
120	3400	830.784344

Table 4.1.: Required time through partitioning

So as displayed, as the partitioning is increased equally in price and volatility, in order to maintain numerical stability the partitioning in time must be increased dramatically, leading

to the very steep evolution in the time to achieve the result. And so in face of the trade-off, when in need of values in between existing mesh points methods such as interpolating between existing values might be more viable for already dense meshes.

4.2. Performance enhancement

The method offers the possibility of including two performance enhancers for a fixed set of parameters, the starting point for b^0 and the tolerance. For starting point, setting it up at higher values allows a lesser number of iterations (and less computation time), with no harm to the final output, although requiring to guess beforehand how big can the b^0 be set. As for the tolerance, as slightly observed in the benchmarking it can be set to make the iteration faster but allowing the exercise barrier to obtain lower values and, therefore, admitting erroneous pricing. The tests performed in this section also use the same parameters of the the stability section, with $l = 400$ and $m = n = 40$.

For the boundary knowing beforehand that lowest barrier point is at $S = 3$, by changing the starting point progressively by the $\delta_x = 0.5$ until 3 it is had:

b^0	Runtime	Iterations per τ
1.0 (baseline)	5.356751	7.8175
1.5	4.989965	7.4275
2.0	4.949008	7.4250
2.5	4.926326	7.4025
3.0	4.410417	6.4075

Table 4.2.: Runtime on b^0

As seen, the performance tends to increase due to the reduction in average number of iterations at each τ, although the progress tends not to be linear, being affected by different behaviours of the appearance the $\frac{\partial p}{\partial x} > -1$ condition.

With respect to the tolerance, setting it up again defined by a γ factor that weights the tolerance for a Spot vector with δ_s depth $\sum b^{n+1} - b^n > (n+1) \times \delta_s \times \gamma$ various values of gamma can be tested:

γ	Runtime	Iterations per τ
0 (baseline)	5.356751	7,8175
0.25	4.568914	6.2925
0.5	4.269172	5.5225
0.75	4.143832	5.2600
1	4.016829	4.8375
1.25	3.906026	4.5400
1.5	3.753894	4.2575
1.75	3.653401	3.9525
2	3.535180	3.6125

Table 4.3.: Runtime on γ

The previous table highlights that the increases in the γ factor increases the computational performance of the numerical method, although this kind of enhancement is not innocuous as the values tend to be affected through undershooting the boundary.

A few cases show the magnitude of this mispricing for γ cases:

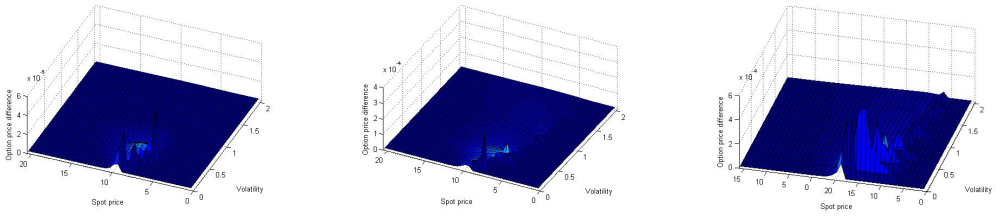

(a) $\gamma = 0.25$ (b) $\gamma = 1$ (c) $\gamma = 2$

Figure 4.1.: Price differences in relation to $\gamma = 0$

As observed, for $\gamma = 0.25$ the difference is negligible, while for the following cases the difference enlarges, reaching wide discrepant differences at $\gamma = 2$. This is justified by the tolerance allowing to miss the boundary, as shown below.

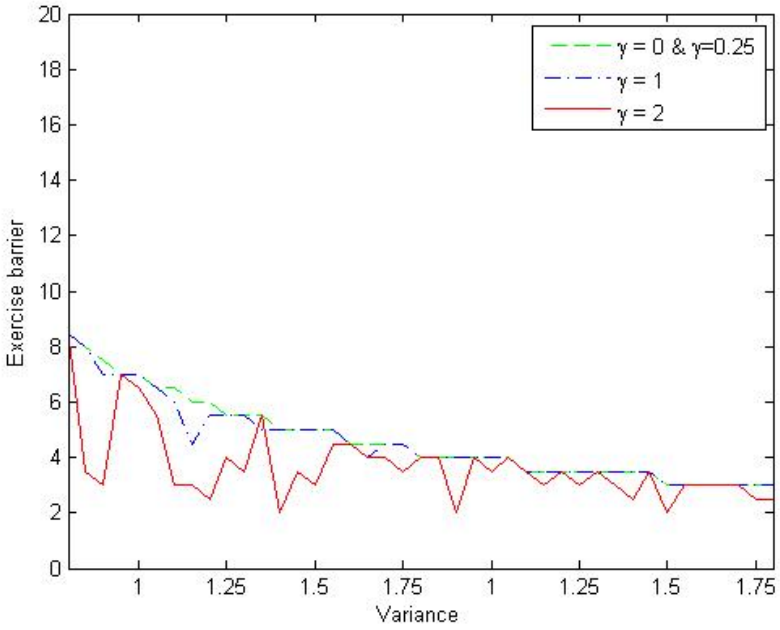

(a) Boundaries difference

Figure 4.2.: γ=0.25

The boundary is the same for $\gamma = 0$ and $\gamma = 0.25$, with the small price differences being justified by the occasional small boundary errors at precedent τ levels, for $\gamma = 1$ the boundary shows some differences, and some variations not conforming to the notion that it should decrease as volatility increases, while for the last case the boundary shows completely erroneous behaviour, far from what one would consider a viable pricing method.

5. Conclusions

In this thesis, first a baseline finite differences approach based on the Heston PDE was used to calculate the price of European options, initially deducting the PDE from the stochastic processes it is based upon, and then implementing it in a finite differences setting, with the results being tested in terms of stability and convergence. After that the model was adapted to calculate the price of American options using a transformation procedure which was presented and described, then proven its effectiveness (although some special cases for the second derivative seem to not align with the general conclusion) and an illustration of its inner procedures was presented. Then the method was used to study different phenomena when altering the used parameters that reflect distinct real world situations, and eventually the method efficiency was studied when different parameters are used.

From its iterated approach focused on the derivative in regards to the underlying asset spot price variable the method proved to be capable of replicating the results of alternative methods, with the likeness dependent on the calibration used, that can increase the computation performance although with repercussions is the achieved price output.

For various sets of variables the method is also responsive to different parameters, being able to manifest the behaviour one would expect in accordance to financial theory and empirical data for given changes in inputs, while in addition showing the effects one would expect when contrasted to the constant volatility setting.

A. Matlab Code for American Options Through Transformation Procedure

```
function [iterations priceput] = TransformationAmerican(parts,
params,K,r,q,S,V,T,p0,tol)

%suggested parameters for testing: ([40 40 400],[3 0.2 0.5 -0.10],
%10,0.02,0,20,2,0.125,1,0)
tic
% Heston parameters
kappa = params(1);
theta = params(2);
sigma = params(3);
rho   = params(4);
lambda = params(5);

% Length of stock price, volatility, and maturity vectors
NS = parts(1)+1;
NV = parts(2)+1;
NT = parts(3)+1;
%Maxima and minima for each variable
Smin = 0;  Smax = S;
Vmin = 0;  Vmax = V;
Tmin = 0;  Tmax = T;

% Increment for Stock Price, Volatility, and Maturity
ds = S/parts(1);
```

```
dv = V/parts(2);
dt = T/parts(3);

% Initialize the 2-D grid with zeros
U = zeros(NS,NV);

% Temporary grid for previous time steps
u = zeros(NS,NV);

% Barrier starting point
%(does not include the last NV, copy from NV-1)
Bnd0=ones(NT-1,NV)*(p0);
% Grid for put exercise prices
for s=1:NS
for v=1:NV
ExeGrid(s,v) = max(K-((s-1)*ds), 0);
end
end

% Boundary condition for t = Maturity
U=ExeGrid;
%Key to check correctly the boundary move at each time
%and volatility point when verifying the derivative
BndKey=ones(NT-1,NV-1);
%Key to indentify if in the first iteration in each tau
IterKey=ones(1,NT-1);
%Starting value for updated boundary
BndAct=ones(NT-1,NV)*(10);
%start global iterations counter
iter=0;
for t=1:NT-1
while (-sum(Bnd0(t,:))+sum(BndAct(t,:)))>(tol)
iter=iter+1;
%Update the boundary
if IterKey(1,t)==0
Bnd0(t,:)=BndAct(t,:);
```

```
end
% Update the temporary grid u(s,t) with the boundary conditions
u = U;

%Update boundary condition for Vmin
for s=2:NS-1
if (s-1)*ds<=Bnd0(t,1) %Exercise below the boundary
U(s,1)=ExeGrid(s,1);
else

if IterKey(t)==1
U(s,1) =u(s,1)*(1 - r*dt - kappa*theta*dt/dv)...
+ dt*(0.5*(r-q)*(s-1)*(u(s+1,1) - u(s-1,1))) ...
+ kappa*theta*(dt/dv)*u(s,2);
end

%Find the last value where px<-1
if BndKey(t,1)==1 && (diff(U(s-1:s,1))/ds)>-1
BndAct(t,1)=(s-2)*ds;
BndKey(t,1)=0;
end
end
end
% Update interior points of the grid (non boundary).

for s=2:NS-1
for v=2:NV-1

if (s-1)*ds<=Bnd0(t,v)%Exercise below the boundary
U(s,v)=ExeGrid(s,v);
else

if IterKey(t)==1
A = (1 - dt*(s-1)^2*(v-1)*dv - sigma^2*(v-1)*dt/dv - r*dt);
B = (1/2*dt*(s-1)^2*(v-1)*dv - 1/2*dt*(r-q)*(s-1));
C = (1/2*dt*(s-1)^2*(v-1)*dv + 1/2*dt*(r-q)*(s-1));
```

```
D = (1/2*dt*sigma^2*(v-1)/dv - 1/2*dt*kappa*(theta-(v-1)*dv)/dv)
+(dt*lambda*sigma*sqrt(v-1));
E = (1/2*dt*sigma^2*(v-1)/dv + 1/2*dt*kappa*(theta-(v-1)*dv)/dv)
-(dt*lambda*sigma*sqrt(v-1));
F = 1/4*dt*sigma*(s-1)*(v-1)*rho;

U(s,v) =A*u(s,v) + B*u(s-1,v) + C*u(s+1,v)...    % The PDE
+ D*u(s,v-1) + E*u(s,v+1)...
+ F*(u(s+1,v+1)+u(s-1,v-1)-u(s-1,v+1)-u(s+1,v-1));
end
%Find the first value where px>-1
if BndKey(t,v)==1 &&(diff(U(s-1:s,v))/ds)>-1
BndAct(t,v)=(s-2)*ds;
BndKey(t,v)=0;
end
end
end
end
%Smax border
U(NS,:)=U(NS-1,:);
%Vmax border
U(:,NV)=U(:,NV-1);
%Update the keys
IterKey(1,t)=0;
BndKey(t,:)=1;
end
%UA(:,:,t)=U(:,:);
end

priceput=U;
iterations=iter;

toc

end
```

Bibliography

[1] Bates D. S., *Jumps and Stochastic Volatility: Exchange Rate Processes Implicit in Deutsche Mark Options* , Review of Financial Studies, 9 (1996), pp. 69-107.

[2] Black F., Scholes M., *The pricing of Option and Corporate Liabilities.* The Journal of Political Economy 81 (1973), pp. 637-654.

[3] Breeden, D. T., *An Intertemporal Asset Pricing Model with Stochastic Consumption and Investment Opportunities .* Journal of Financial Economics 7 (1979), pp. 265-296.

[4] Chockalingam, A., Muthuraman. K., *American Options Under Stochastics Volatility.*, Operations Research, 59 (2011), pp. 793-809.

[5] Clarke, N., Parrott, K., *Multigrid for American Option Pricing with Stochastic Volatility* , Applied Mathematical Finance, 6 (1999), pp. 177-195.

[6] Cox, J. C., Ross S. A., *The Valuation of Options for Alternative Stochastic Processes* , Journal of Financial Economics, 3 (1976), pp. 145-166.

[7] Heston, S. L., *A Closed-form Solution for Options with Stochastic Volatility and Applications to Bond and Currency Options.* Review of Financial Studies 6(2) (1993), pp. 327-343.

[8] Hull, J., White. A., *The Pricing of Options on Assets with Stochastic Volatilities.*, The Journal of Finance, 42 (1987), pp. 281-300.

[9] Ikonen, S., J. Toivanen, *Componentwise Splitting Methods for Pricing American Options under Stochastic Volatility* , International Journal Theoretical Applied Finance, 10 (2007a), pp. 331-361.

[10] Ikonen, S., J. Toivanen, *Efficient Numerical Methods for Pricing American Options Under Stochastic Volatilityy* ,Numerical Methods for Partial Differential Equations, 24 (2007b), pp. 104-126.

[11] IN 'T HOUT K. J., FOULON S., *ADI Finite Difference Schemes for Option Pricing in the Heston Model with Correlation* , International Journal of Numerical Analysis and Modelling , 7 (2010), pp. 303-320.

[12] MELINO, A., TURNBULL. S. M., *Pricing Foreign Currency Options with Stochastic Volatility.*, Journal of Econometrics, 45 (1990), pp. 239-265.

[13] MELINO, A., TURNBULL. S. M., *Misspecification and the Pricing and Hedging of Long-Term Foreign Currency Options.*, Journal of International Money and Finance, 14 (1995), pp. 373-393.

[14] SCOTT, L. O., *Option Pricing When the Variance Changes Randomly: Theory, Estimation, and an Application*, Journal of Financial and Quantitative Analysis, 22 (1987), pp. 419-438.

[15] STEIN, E. M., AND STEIN J. C., *Stock Price Distributions with Stochastic Volatility: An Analytic Approach*, Review of Financial Studies, 4 (1991), pp. 727-752.

[16] WIGGINS, J. B., *Option Values under Stochastic Volatilities*, Journal of Financial Economics, 19 (1987), pp. 351-372.